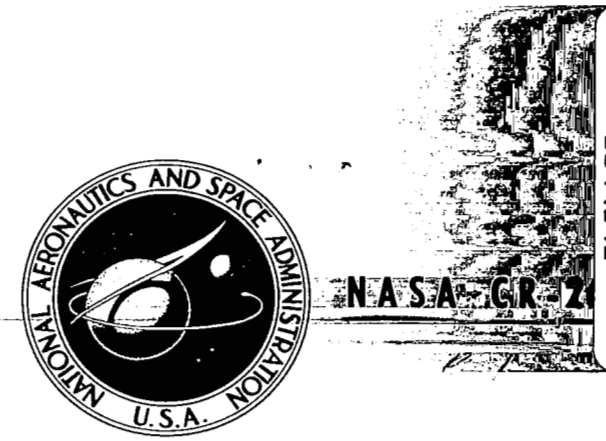

NASA CONTRACTOR REPORT

NASA CR-264

INLET-TO-INLET SHOCK INTERFERENCE TESTS

by D. L. Motycka aud J. B. Murphy

Prepared under Contract No. NAS 2-2079 *by*
UNITED AIRCRAFT CORPORATION
Pratt & Whitney Aircraft Division
East Hartford, Conn.
for
NATIONAL AERONAUTICS AND SPACE ADMINISTRATION • WASHINGTON, D. C. • SEPTEMBER 1965

NASA CR-264

INLET-TO-INLET SHOCK INTERFERENCE TESTS

By D. L. Motycka and J. B. Murphy

Prepared under Contract No. NAS 2-2079 by
UNITED AIRCRAFT CORPORATION
Pratt & Whitney Aircraft Division
East Hartford, Conn.

for

NATIONAL AERONAUTICS AND SPACE ADMINISTRATION

For sale by the Clearinghouse for Federal Scientific and Technical Information
Springfield, Virginia 22151 – Price $3.00

FOREWORD

This final report describes the work which was accomplished by Pratt & Whitney Aircraft for NASA Ames Research Center in accordance with the requirements defined by Contract NAS2-2079 entitled "Inlet-to-Inlet Shock Interference Tests", dated June 30, 1964. This report has been prepared to fulfill the requirements of Article IX (C) of the subject contract.

TABLE OF CONTENTS

ILLUSTRATIONS

ILLUSTRATIONS (Cont'd)

TABLES

LIST OF SYMBOLS

A	Flow area
A_1	Physical cowl-lip capture area
A_o	Capture flow area at free stream conditions
A_P	Internal passage area
g	Gravitational constant = $32.2 \frac{\text{ft lb}}{\text{lb sec}^2}$
A_o/A_1	Overall mass flow ratio
A_3/A_o	Contraction ratio = $\frac{A_3/A_1}{m_i/m_o}$
M	Mach number
$\mathring{m}$	Mass flow function, $\frac{Wa\sqrt{T_T}}{P_s A} = \sqrt{\frac{\gamma g}{R'}} \; M \left[1 + \frac{\gamma-1}{2} M^2\right]^{1/2}$
$\bar{m}$	Mass flow function, $\frac{Wa\sqrt{T_T}}{P_T A} = \sqrt{\frac{\gamma g}{R'}} \; M \left[1 + \frac{\gamma-1}{2} M^2\right]^{-\frac{\gamma+1}{2(\gamma-1)}}$
$\bar{m}_*$	$\bar{m}$ value at Mach number 1.0, equals 0.5318
m_{bl}/m_o	Boundary layer bleed flow
m_i/m_o	Mass flow ratio at subsonic diffuser exit
P	Upstream inlet throttle position
P_P	Pitot pressure, local
P_S	Static pressure
P_T	Total pressure, average
Q	Flow coefficient
R	Radius measured from model axis

R'	Gas constant for air = 53.3 ft lb/lb °R
Re_{D_1}	Reynolds number based on inlet cowl lip diameter
S	Balance throttle position (used for downstream inlet)
T_T	Total temperature
Wa	Actual airflow
X	Axial distance measured from tip of centerbody
X_C	Axial distance measured from tip of centerbody to cowl lip leading edge
Z	Distance from cowl lip
γ	Ratio of specific heats for air = 1.4
θ	Angle in degrees measured from the plane of the expelled shock cowl lip to the closest point on the adjacent inlet cowl lip (see Figure 30)
θ_c	Centerbody initial half angle
θ_s	Conical shock half angle
ψ	Radial distance between pods measured in units of inlet diameters

Subscripts Apply to the Above Symbols

o	Free stream conditions
1	Capture cowl lip station
3	Inlet throat
7	Compressor face station
8	Plenum at aft end of model
9	Balance throttle throat station
D or DSI	Downstream inlet
U or USI	Upstream inlet

ABSTRACT

As flight speeds increase, supersonic aircraft powerplant installations may encounter complex aerodynamic problems due to shock reflection and the possibility of inlet shock instability created by pod-to-pod interference. This report describes the experimental program conducted and presents wind tunnel test data obtained during a comprehensive study of adjacent inlet interference. This test program established, for a typical Mach 3.0 design mixed compression inlet, the dividing line between the regions of expelled shock interference and completely stable operation. A study was also conducted to determine the effect of placing a plate between pods.

SUMMARY AND CONCLUSIONS

The results of this experimental program can be summarized as follows:

1. It is possible to operate a mixed compression inlet in the region of influence of another inlet which is "buzzing", but it must be operated at a reduced contraction and hence a reduced total pressure recovery.

2. The pressure recovery penalties encountered were large for steady state operation behind the "buzzing" inlet, but the penalty required to maintain stability during the initial transient of the onset of "buzz" was so severe that it cannot be considered practical.

3. The line of demarcation between the regions of stable and unstable operation was found to approximately coincide with the shape of the expelled "buzzing" shock in its maximum forward position.

4. The pressure recovery penalties encountered while operating in the unstable region behind the expelled shock were reduced as the distance between the inlet cowl lip and the source of the expelled shock was made very large. The penalties were also reduced as the Mach number was reduced.

5. The use of a plate as an interference shield was very effective in eliminating the penalty imposed by the expelled shock.

6. The magnitude of the initial pressure pulse at the onset of "buzz" is the same as it is for subsequent cycles.

7. The "buzz" frequency increased as model airflow was reduced (throttled) but the pressure impulse amplitude remained approximately constant.

8. The basic "buzz" frequency was dependent upon the volume in the model between the cowl lip and the choked throttle rather than the volume from the cowl lip to the throat of the inlet.

INTRODUCTION

Inlet development for supersonic aircraft presents many problems to both airframe and engine manufacturers. A thorough investigation of all performance penalties associated with the various types of air induction systems must be undertaken before the proper engine spacing can be selected. One of these penalties could come from the safety factors needed to overcome inlet-to-inlet interference effects.

For many applications the podded powerplant concept rather than the airframe integrated system has many favorable features. However, individually podded engine configurations on a supersonic aircraft can experience shock interference between adjacent inlets. Inlet instability may result which could prove severe enough to create a critical flight condition. Oscillations of the inlet expelled shock wave could be created which may cause a flameout or damage the engine. Furthermore the oscillating shock may adversely affect an adjacent inlet. Safety factors incorporated for the purpose of preventing inlet-to-inlet interference result in a thrust loss and an increase in the specific fuel consumption. Economics demand that any penalties be eliminated or minimized. The program undertaken was designed to establish the pressure recovery penalties for operating a supersonic inlet in the flow field of an adjacent subcritical inlet, and to establish the non-interference envelope.

A very preliminary program, reported in Pratt & Whitney Aircraft TDM-1753, entitled "The Effect of an Interference Shock on the Performance of a Mach 3.0 Axisymmetric Moveable Centerbody Inlet", provided some insight into inlet performance penalties which can occur when podded powerplants are not properly aerodynamically positioned. A more comprehensive program which better defines these inlet-to-inlet shock interference effects has been studied under the subject contract.

The parameters investigated include the total pressure recovery at the compressor face, inlet mass flow, and inlet contraction ratio for various pod-to-pod axial and lateral spacings. In addition, "buzz" frequency and pressure amplitude were measured. The possibility of using a plate placed between adjacent pods as a means of reducing

shock interference effects was also investigated. Testing was accomplished by using two inlets operating simultaneously in the United Aircraft Corporation Research Laboratories 17 inch x 17 inch supersonic wind tunnel facility between Mach numbers 2.0 and 3.0. The Reynolds numbers based on the inlet capture diameter, R_{eD_1}, in the wind tunnel test section is shown in Figure 1.

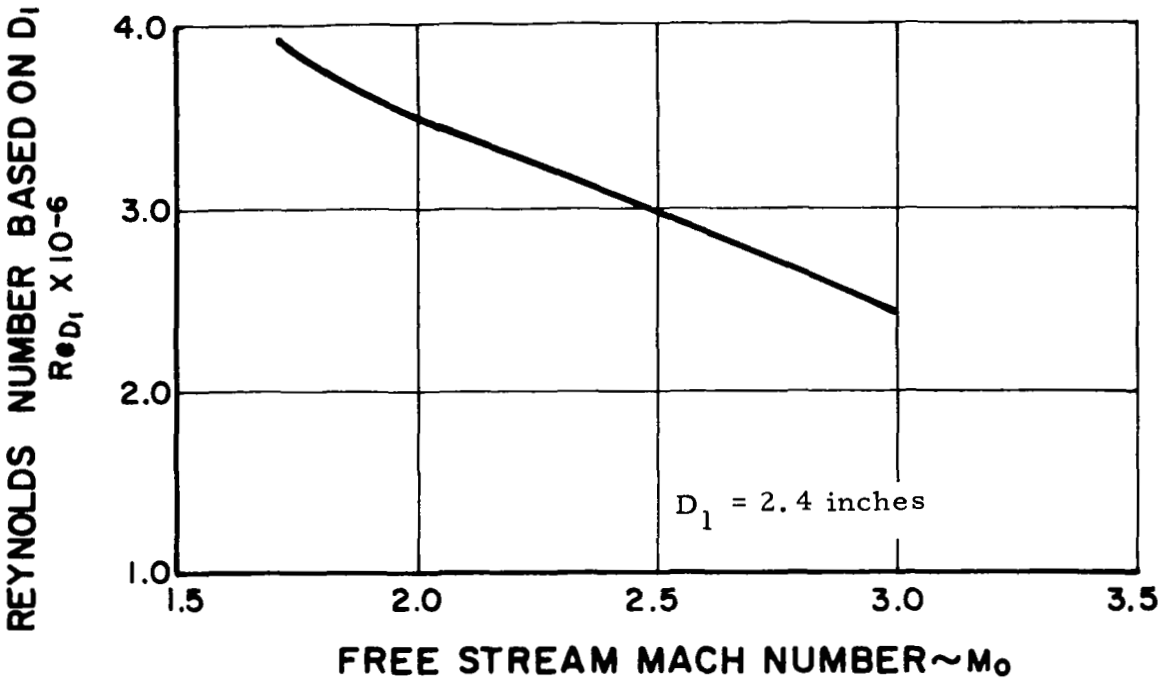

Figure 1. Variation of Wind Tunnel Reynolds Number with Free Stream Mach Number

DESCRIPTION OF MODELS

Model Geometry

Two axisymmetric mixed compression inlet models designed for Mach 3.0 cruise operation were selected for this experimental program, (see Figure 2). These inlets were scaled down versions of a previously calibrated axisymmetric mixed compression inlet having an airflow schedule compatible with the demands of a typical turbojet airflow schedule. They were 2.4 inches in cowl lip diameter with initial half cone angles of 12 degrees followed by a gradual amount of contraction to the throat. Figure 2 is a photograph of the inlets mounted in the wind tunnel with the cowls removed to show the construction details. A centerbody ram type scoop was used on both inlets for removal of the boundary layer from the cone surface. The centerbody bleed flow was collected internally and discharged through four struts directly to the freestream air as seen in Figure 2. This was followed by a nearly constant throat area passage and a divergent subsonic diffuser passage. Figure 3 shows a schematic drawing of the model with tabulated inlet coordinates. The cowl of the downstream inlet model had 15 rows of perforations slanted at an angle of 30 degrees to provide for the removal of boundary layer from the internal surface of the cowl. There were never more than 10 rows utilized at any one time during the program. In the interest of economy, the upstream inlet cowl did not have any bleed perforations as it was felt that the "expelled shock" performance of this inlet would not be materially different with or without the cowl bleed. The performance of the downstream inlet was the most critical for this type of program. With the exception of the cowl perforation bleed the two inlets were identical. Figure 4 shows the ratio of internal passage area to inlet capture area, A_p/A_1, in the Mach 3.0 design position. The variation of throat area ratio, A_3/A_1, as a function of centerbody position, R_1/X_c is shown in Figure 5.

The inlet centerbodies were movable and were actuated by Acme drive screws which in turn were driven by 50 volt miniature motors. The motor movements were controlled by remote servo power positioners through the feedback part of dual helical potentiometers. The indicator half of the potentiometers were connected to the Bristol charts for visual record and then to the encoder for a punch card output. This in turn was fed to the data reduction program.

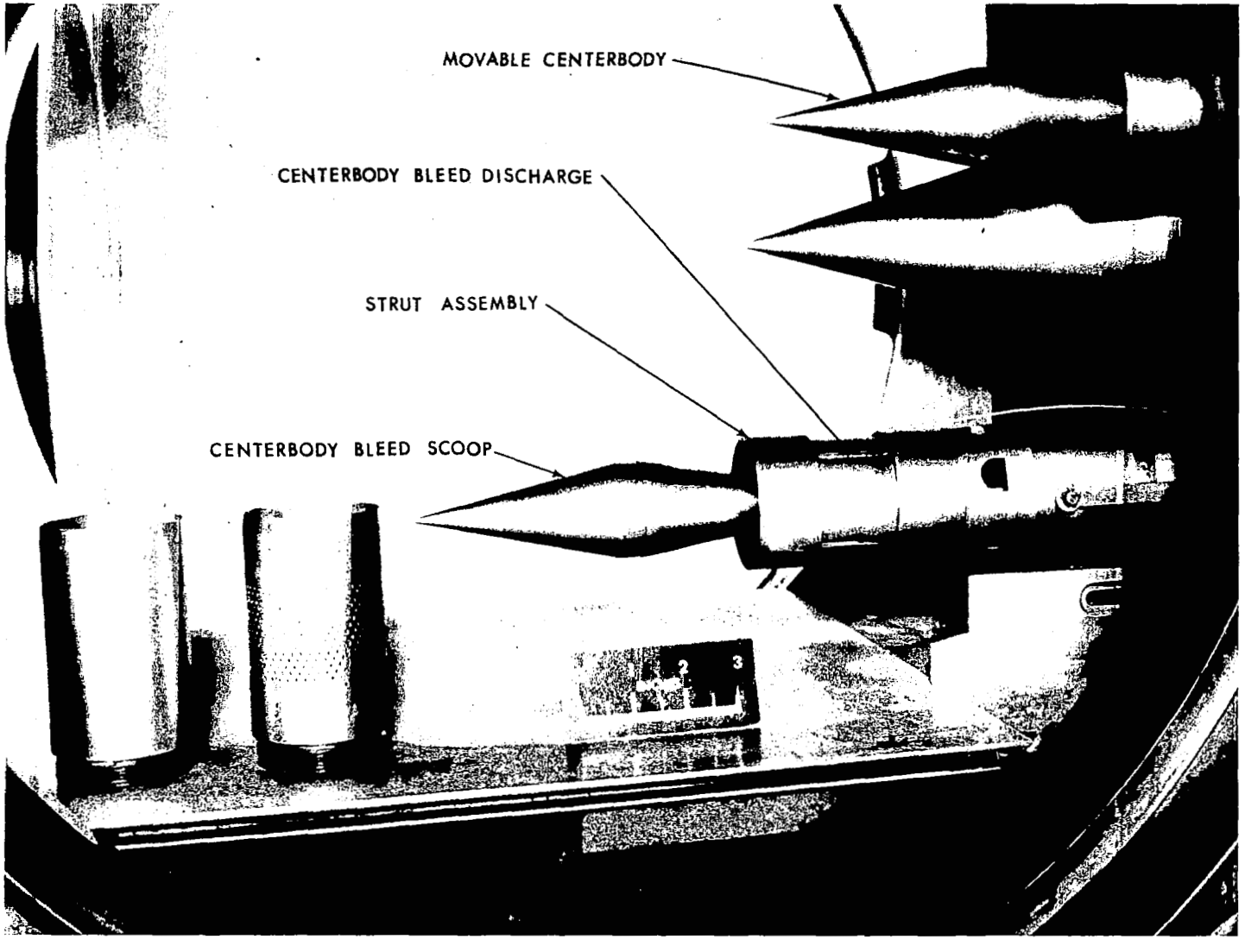

Figure 2. Model Installation in Supersonic Wind Tunnel - Mach 3.0
Centerbody Position with Cowls Removed - ψ = 2.0
Diameters - Θ = 56.5°

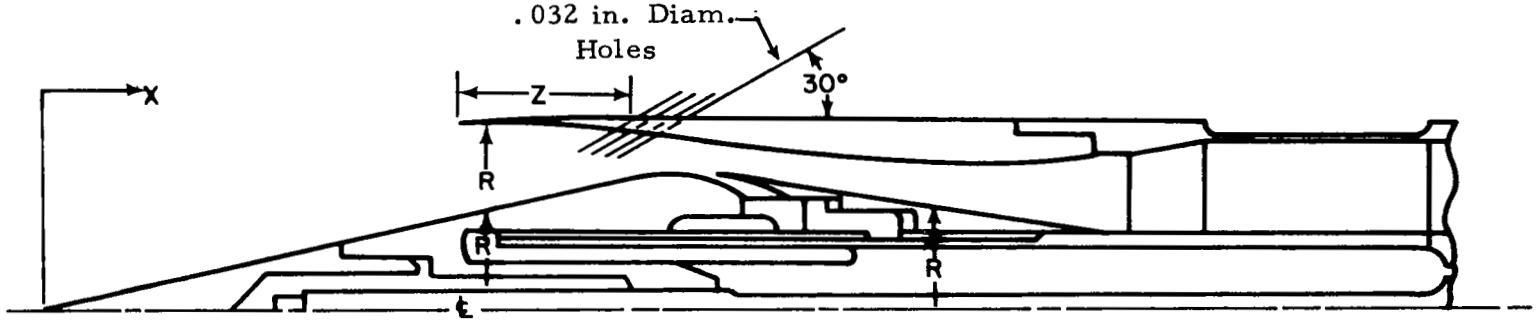

CENTERBODY COORDINATES

X (IN.)	R (IN.)
0	0
STRAIGHT LINE	
3.947	.839
4.043	.853
4.122	.860
4.228	.860
4.333	.858
4.439	.851
4.492	.841
4.465	.849
4.465 B.L. Scoop	.869
4.545	.867
4.677	.852
4.809 Throat	.831
4.941	.808
5.073	.786
5.337	.736
5.601	.692
5.866	.653
STRAIGHT LINE	
6.800 Compressor Face Sta.	.521

COWL COORDINATES

X (IN.)	R (IN.)
2.801 L.E.	1.189
2.986	1.193
3.144	1.194
3.303	1.193
3.514	1.183
3.779	1.160
STRAIGHT LINE	
5.020	1.018
5.258	.989
5.417	.976
5.681	.964
5.945	.959
6.474	.970
7.002	1.011

COWL PERFORATIONS LOCATED AT

Z (IN.)
1.161
1.267
1.373
1.479
1.585
1.691
1.797
1.902
2.008
2.114
2.219
2.325
2.431
2.537
2.642

Figure 3. Inlet Coordinates With Centerbody at Mach 3.0 Design Position

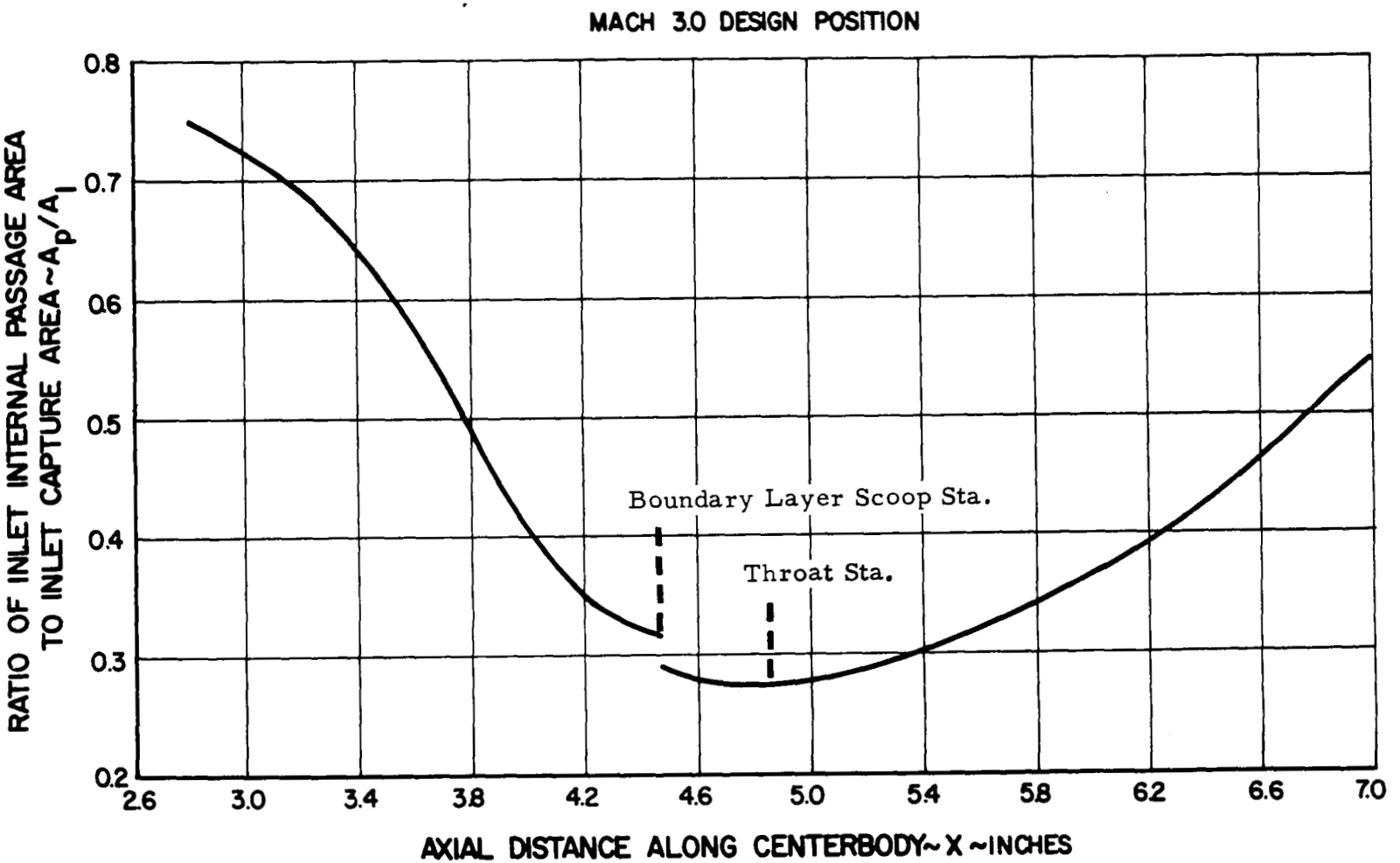

Figure 4. Ratio of Inlet Internal Passage Area to Inlet Capture Area Versus Centerbody Axial Distance Mach 3.0 Design Position

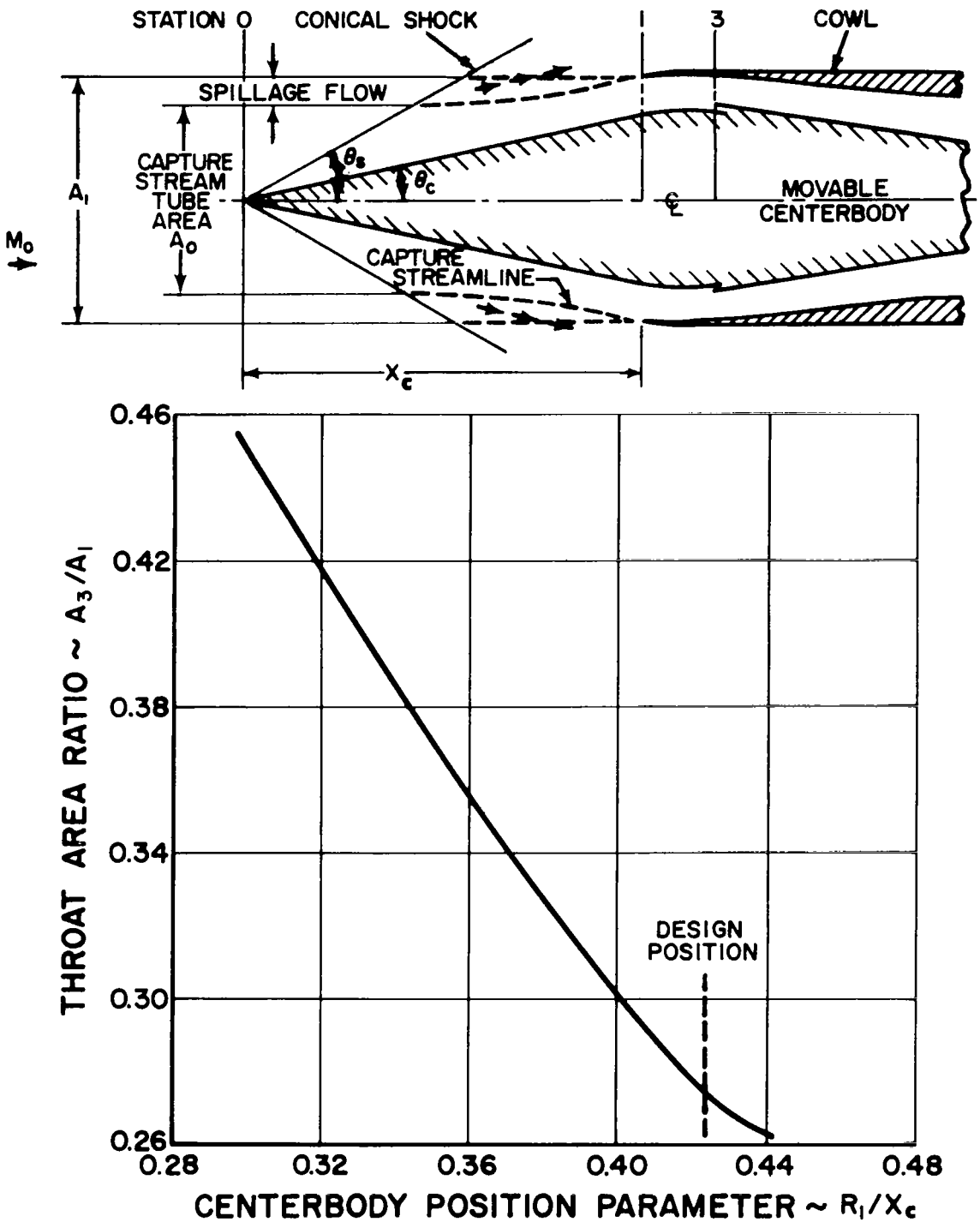

Figure 5. Variation of Inlet Throat Area With Centerbody Position Parameter

Figure 6 shows a photograph of the inlet model components utilized during this program.

The downstream inlet model was attached to a 4.7 inch diameter tunnel shaft by a rotating connection. This type of arrangement allowed the downstream inlet to be throttled normally by the tunnel's movable plug, Figure 7. Rotation of the downstream inlet caused the spacing between the inlet models to vary (see Figure 8). The upstream inlet was attached to the tunnel floor by means of a base plate and track combination. Translation along this track enabled the axial distance between the inlets to be varied. The combinations of the downstream and upstream mounting configurations allowed for an infinite number of positions to be attained for testing the models. An independent method of throttling the upstream inlet was employed. A sleeve arrangement, which slid over the outer surface of the cowl, was driven by a motor encased in the rear section of the upstream model (see Figures 8 and 9). There were six internal air passage discharge ports that were used in conjunction with this throttling device.

A plate was mounted on the upstream inlet to evaluate the feasibility of shielding as shown in Figures 9 and 10. This would enable the downstream inlet to operate normally when a shock was expelled from the adjacent upstream inlet.

Instrumentation

Figures 7 and 8 show the various types of instrumentation employed during the complete experimental program.

The downstream inlet airflow was measured by a calibrated 3 square inch movable plug throttle. The airflow on the upstream model was throttled independently but was not measured. Mass flows for this model were estimated from known centerbody positions and centerbody bleed flows. A pitot rake with three probes and a static tap was installed on the downstream inlet at the compressor face (station 7). Static taps were also placed in both model plenum sections (station 8). A single pitot probe was placed in the centerbody bleed discharge passage of the downstream inlet and in the upstream inlet model at the simulated compressor face.

The pitot probe placed in the centerbody bleed discharge strut was used to calculate the amount of centerbody bleed flow which was bled

off by the ram scoop. This was accomplished by using the following equation:

By continuity,

$$\frac{m_{b1}}{m_o} = \frac{P_{T_{b1}} A_{b1} \bar{m}_{b1} \sqrt{T_{T_o}}}{P_{T_o} A_1 \bar{m}_o \sqrt{T_{T_{b1}}}} Q_{b1}$$

and $T_{T_o} = T_{T_{b1}}$

The bleed flow is assumed to be choked at the discharge exit. $P_{T_{b1}}$, P_{T_o}, A_{b1}, and A_1 are measured quantities and $\bar{m}$ is a function of Mach number. Q_{b1} was estimated at 0.80 based on previous experience with a similar model.

The pitot rake, consisting of three probes, and the static tap located at station 7 of the downstream inlet was used to calculate the average total pressure recovery. Two methods of evaluating the total pressure recovery were used: (1) continuity average total pressure and (2) area weighted average integration. The former method was determined from measurements, at station 7, of the static pressure, of the area, of the airflow, and of the total temperature.

The following relationship illustrates the method of calculating the continuity average total pressure recovery:

The average Mach number at station 7, M_7, must be evaluated before P_{T_7} can be evaluated. Therefore,

$$W_a = \frac{P_{s7} A_7 \dot{m}_7^\circ}{\sqrt{T_{T_7}}}$$

Then $$\dot{m}_7^\circ = \frac{W_a \sqrt{T_{T_7}}}{A_7 P_{s7}}$$

and $\dot{m}_7^\circ$ determines M_7 which, in turn, determines P_{T_7}/P_{S_7}.

Then

$$\frac{P_{T_7}}{P_{T_o}} = \left(\frac{P_{S_7}}{P_{T_o}}\right) \times \left(\frac{P_{T_7}}{P_{S_7}}\right)$$

The latter method, area weighted average integration, was accomplished by integrating the total pressure profile across the passage area.

It was the original intention to use the static pressure in the plenum, station 8, as a measure of total pressure recovery. However, apparently because of higher than expected velocities and a distorted flow profile in the plenum, the total pressure recoveries of both downstream and upstream models were found to be erroneous. Therefore, the pitot probe in the upstream inlet at station 7 was added (serving primarily to determine when the normal shock was expelled) and the rake in the downstream inlet at station 7 was used to determine total pressure recovery.

A static tap at downstream inlet station 7 (different circumferential location than that used to calculate the continuity average total pressure) was used to measure "buzz" frequency and pressure amplitude of the expelled shock by means of a close coupled connection to a differential transducer.

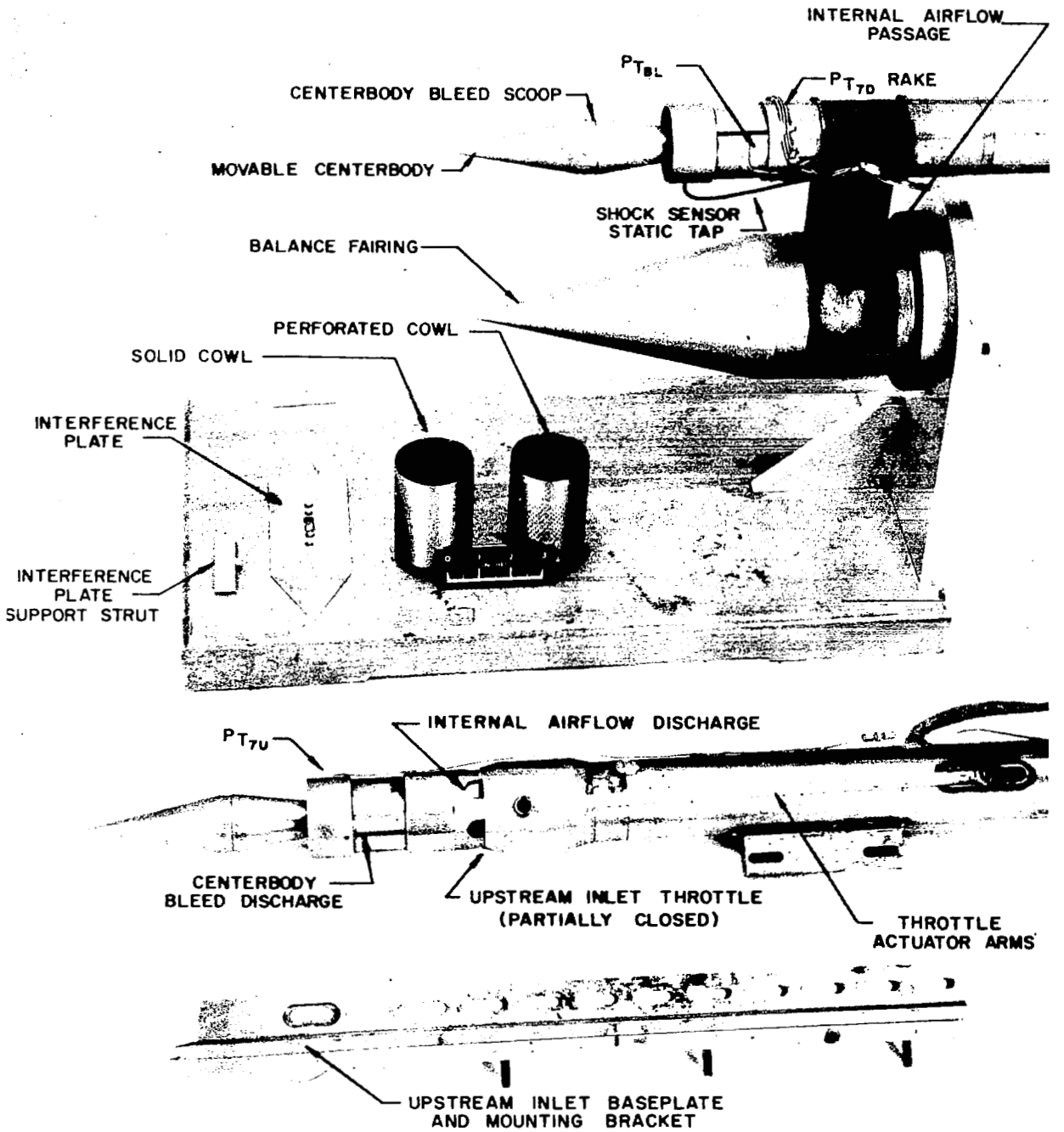

Figure 6. Inlet-To-Inlet Shock Interference Test Model Components

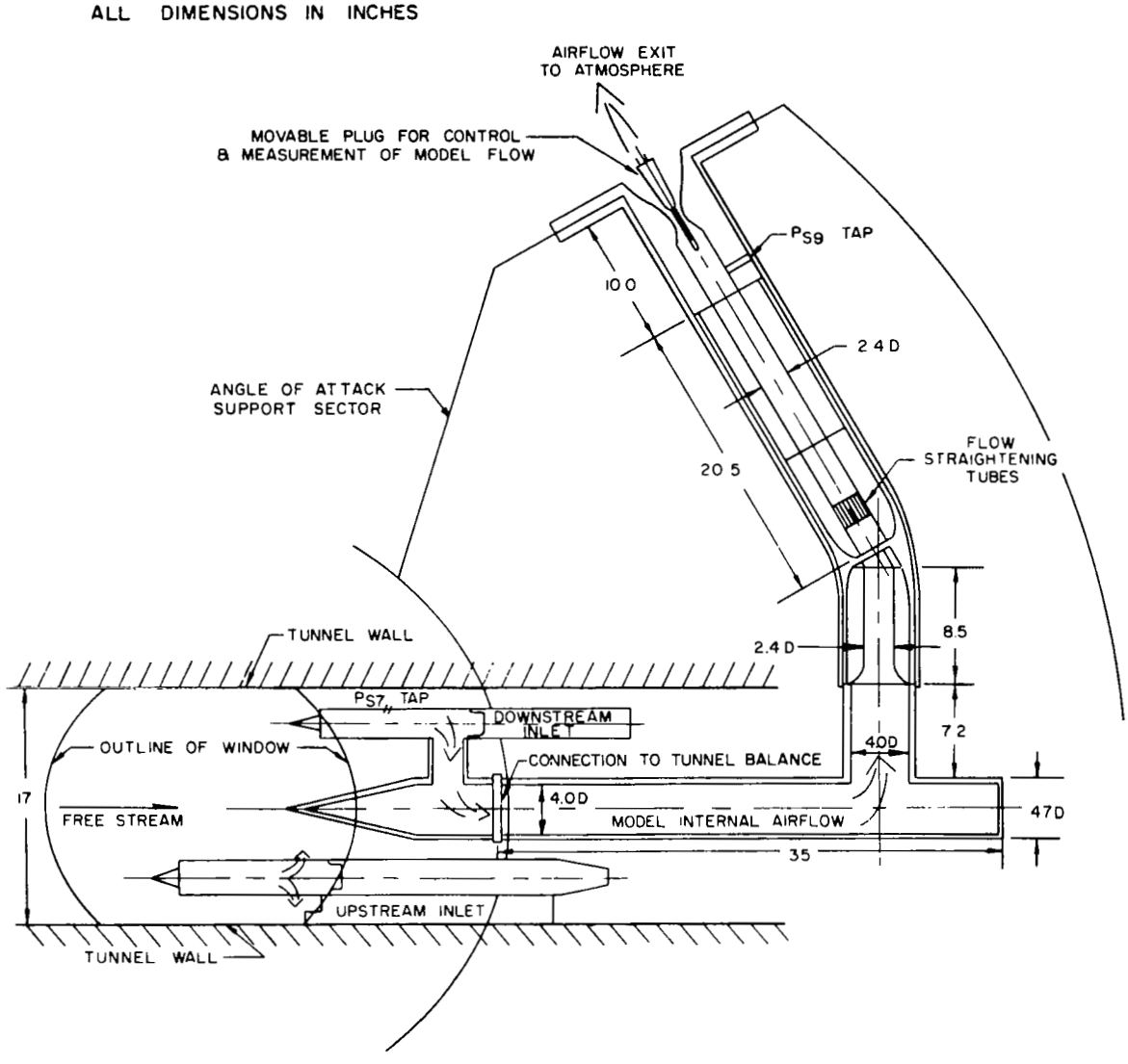

Figure 7. Schematic Diagram of Inlet Airflow Passages

$M_o = 3.0 - \psi = 3.0 \sim \theta = 10°$

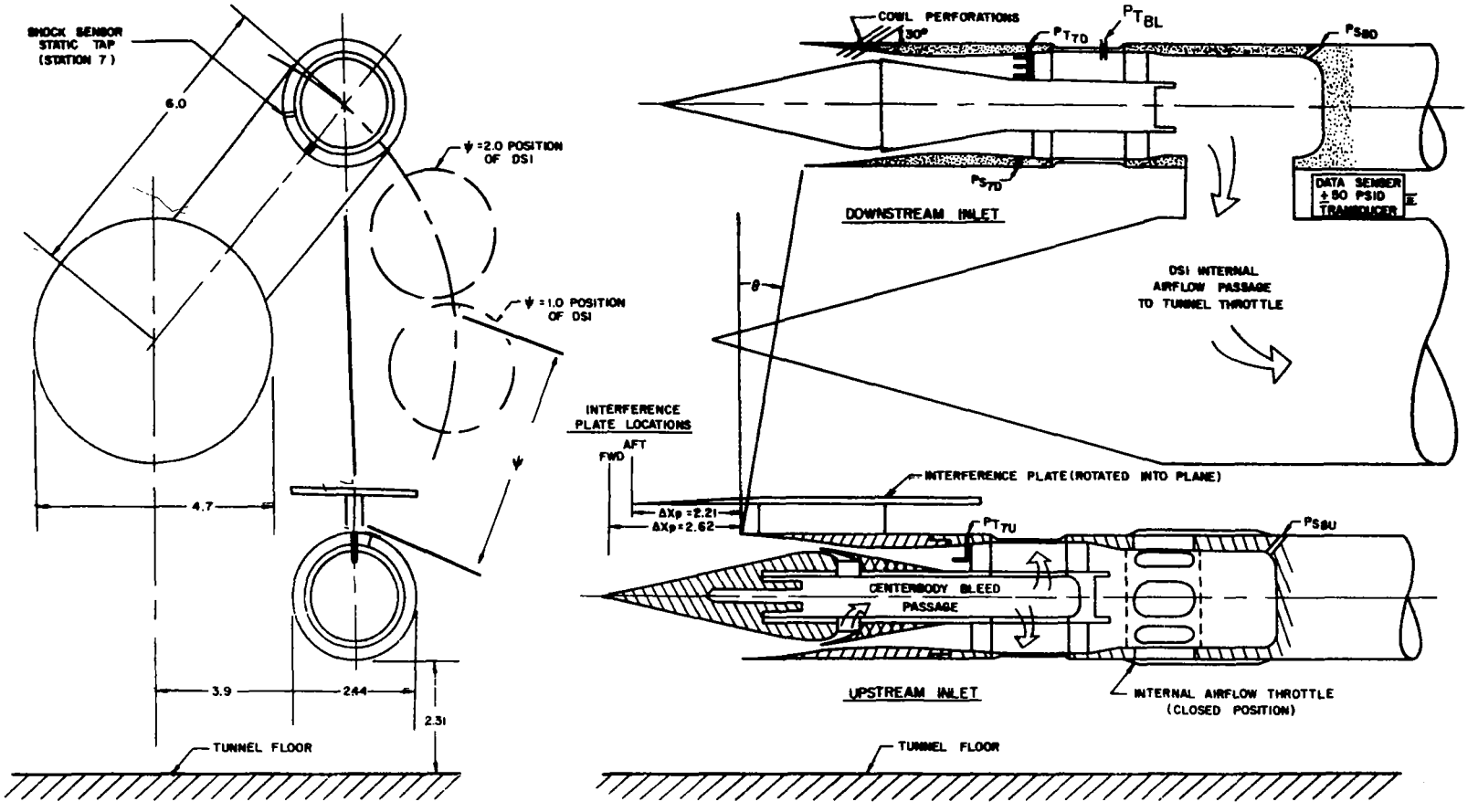

Figure 8. Schematic Drawing of Inlets With Phase I & II Instrumentation

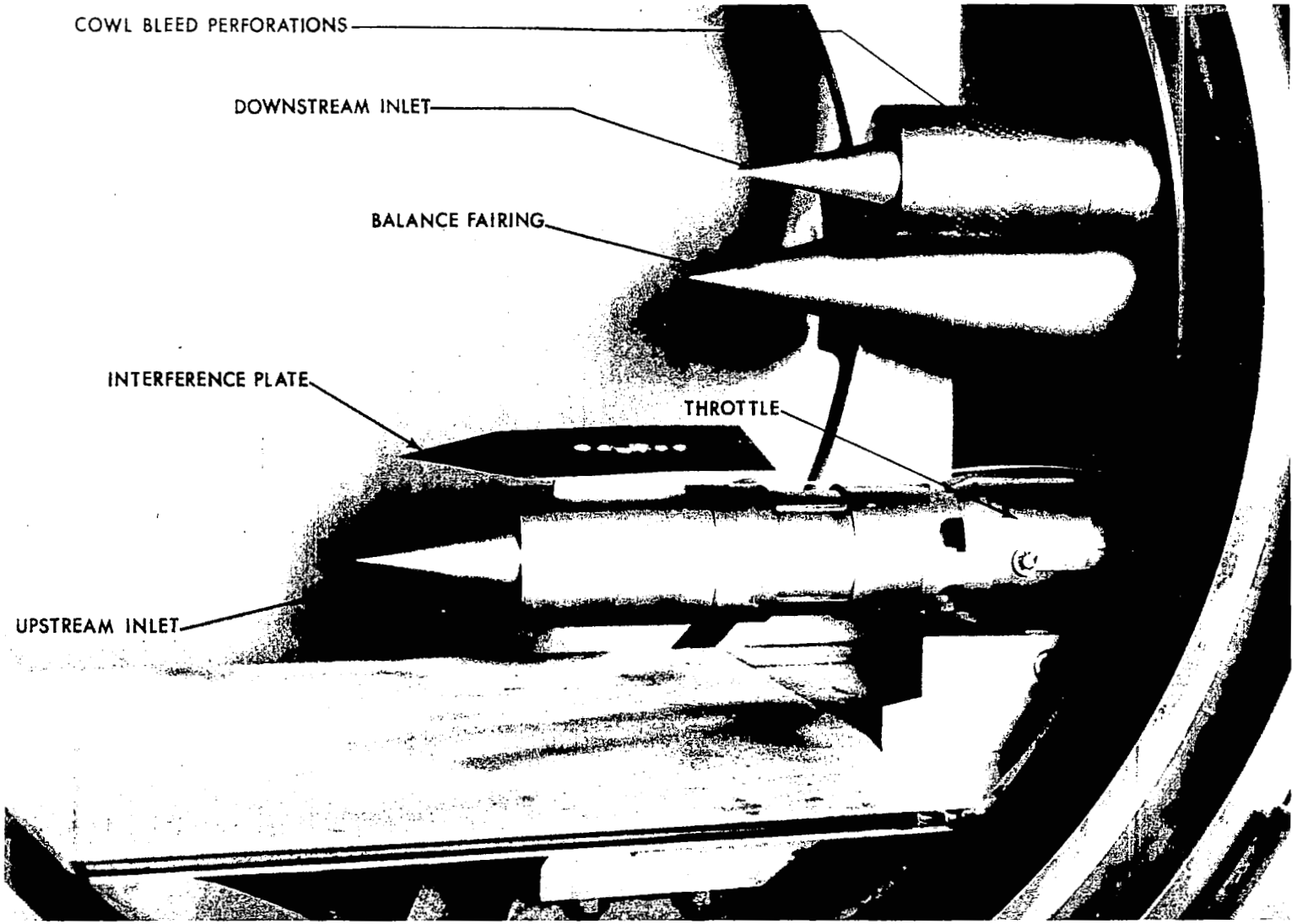

Figure 9. Model Installation in Supersonic Wind Tunnel - Mach 3.0 Centerbody Position-Interference Plate in Aft Position - ψ = 2.0 Diameter - Θ = 56.5°

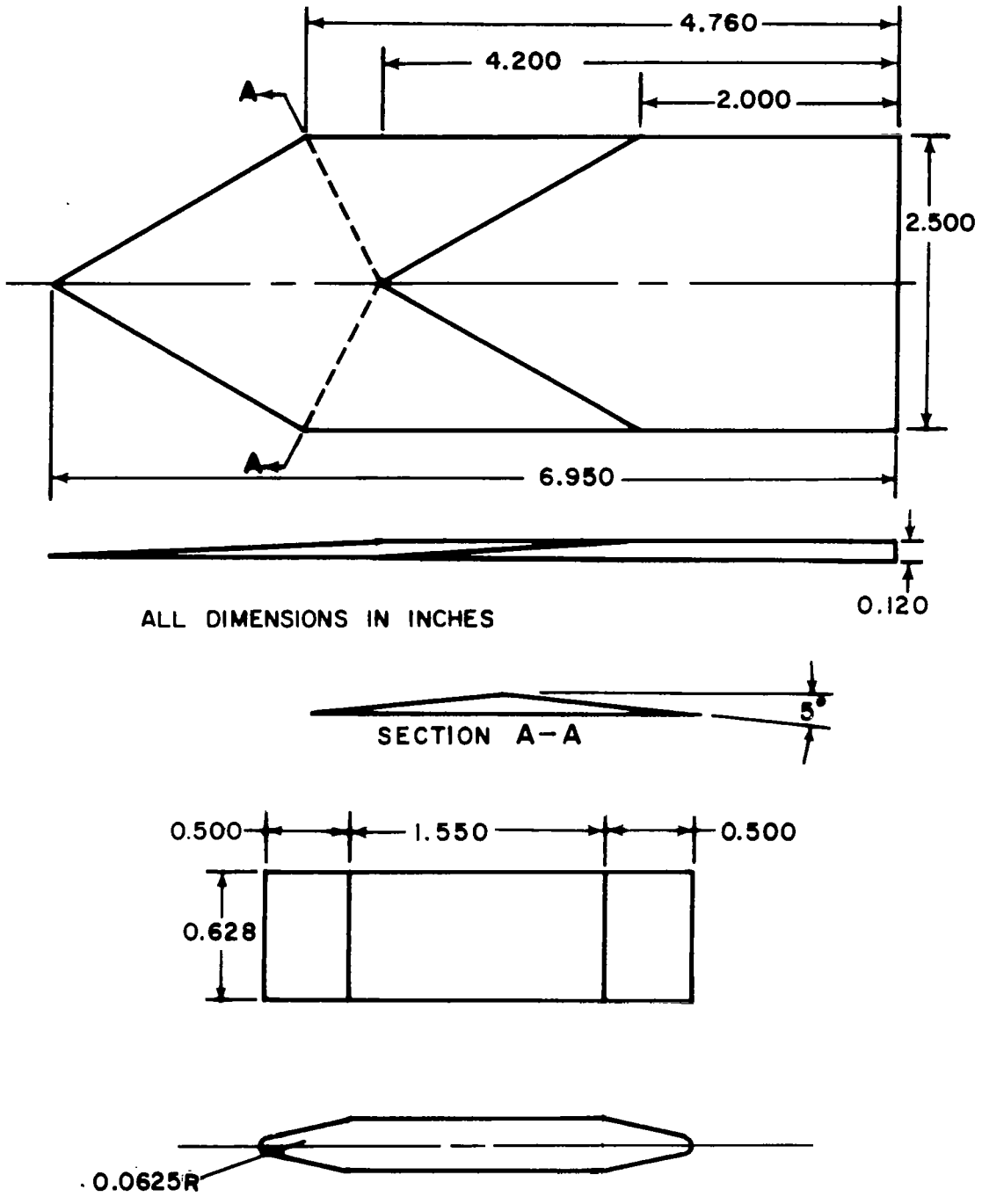

Figure 10. Interference Plate and Support Strut

DESCRIPTION OF TEST EQUIPMENT

1. General Description of 17 Inch Supersonic Wind Tunnel

The tests were conducted in the United Aircraft Laboratories 17 inch x 17 inch intermittent-flow (pressure blowdown) supersonic wind tunnel facility. This tunnel provides a uniform flow at Mach numbers ranging from 1.5 to 5.0. The nozzle, Figure 11, in this tunnel consists of a pair of flexible plate whose contours are adjusted by means of hydraulic jacks. Dry air is supplied to this tunnel at a total temperature of approximately 80° F and at stagnation pressures up to 400 psig. Curves showing the available run time as a function of tunnel stagnation pressure and Mach number are presented in Figure 12. The corresponding Reynolds number envelope is presented in Figure 13.

An inlet mount shaft having an outside diameter of 4.70 inches was utilized. The shaft was mounted on a variable angle-of-attach sector and airflow was ducted through the inlet model and sector cavity to a constant-area section just upstream of a choked flow-measuring bellmouth whose area is varied by a hydraulically operated plug throttle (see Figure 7). Twelve channels of digital information are recorded continuously on strip charts and punched simultaneously into IBM cards at the rate of 100 cards per minute. A complete description of the equipment and procedures available in the supersonic wind tunnel is described fully in reference 6. A single-pass schlieren system, which incorporates a 20 inch parabolic mirror and a schlieren viewing screen, was used for observing and photographing flow characteristics.

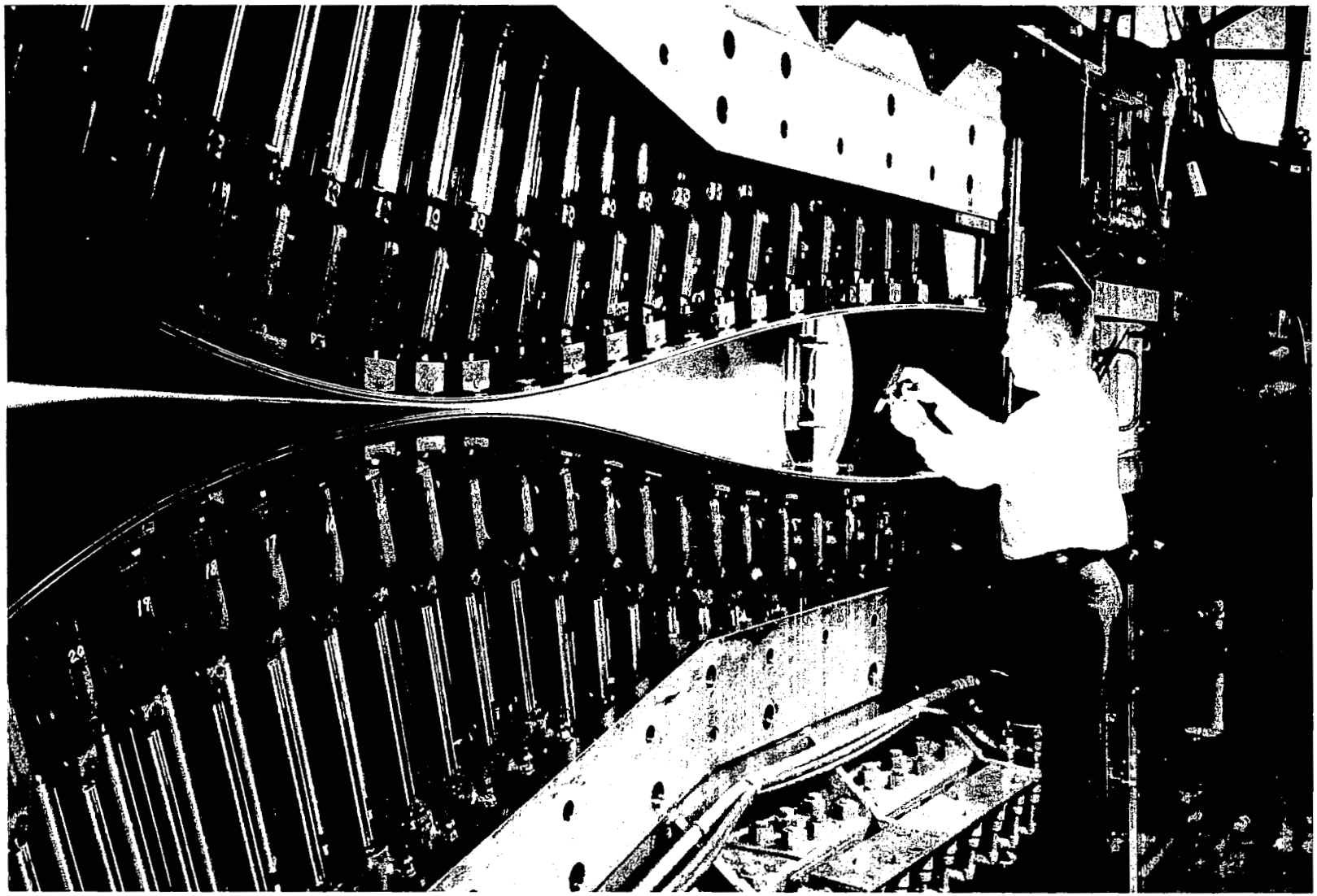

Figure 11. 17 x 17 Inch Supersonic Wind Tunnel - Side Wall Removed to Show Flexible Walls and Actuating Mechanisms

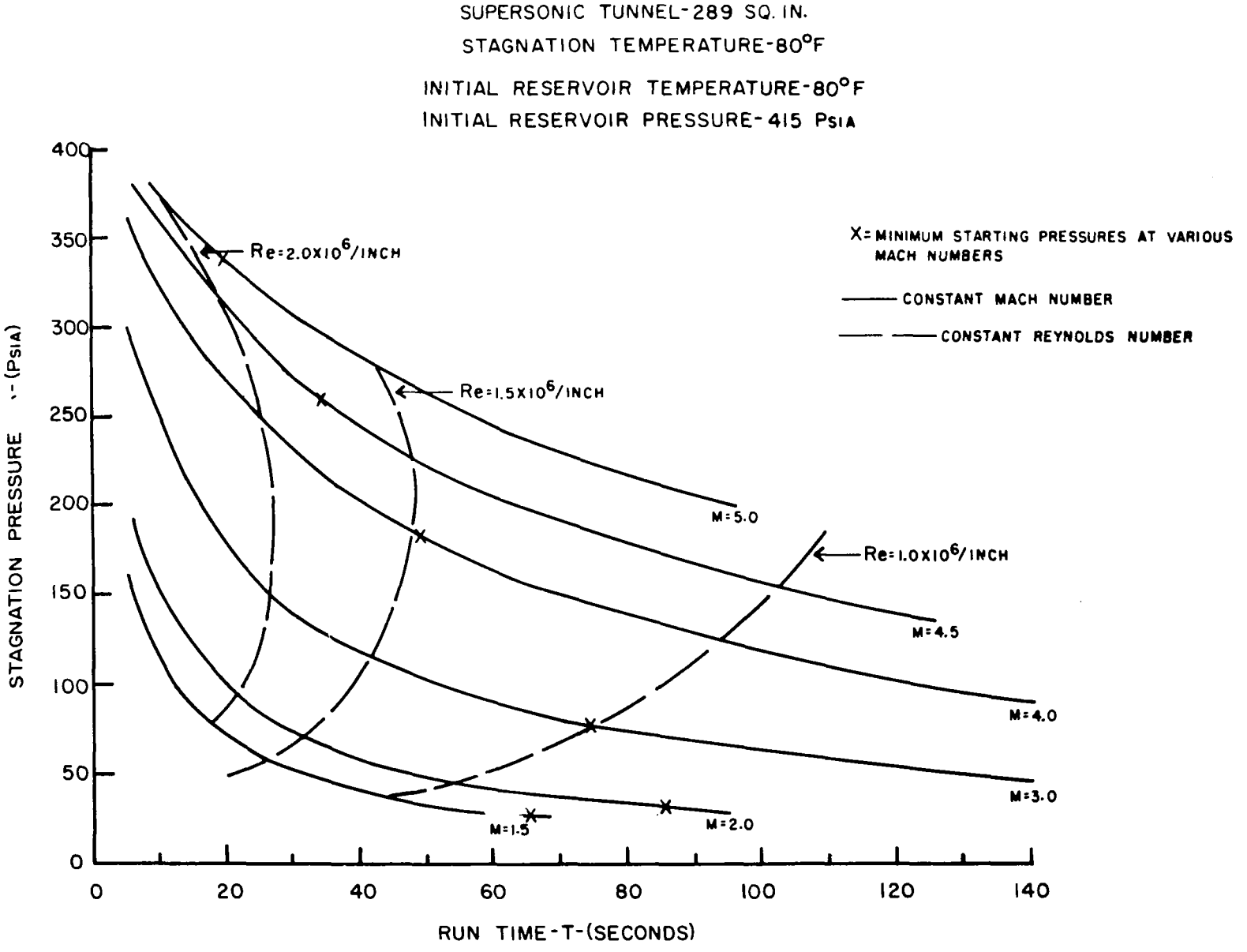

Figure 12. Stagnation Pressure Versus Run Time

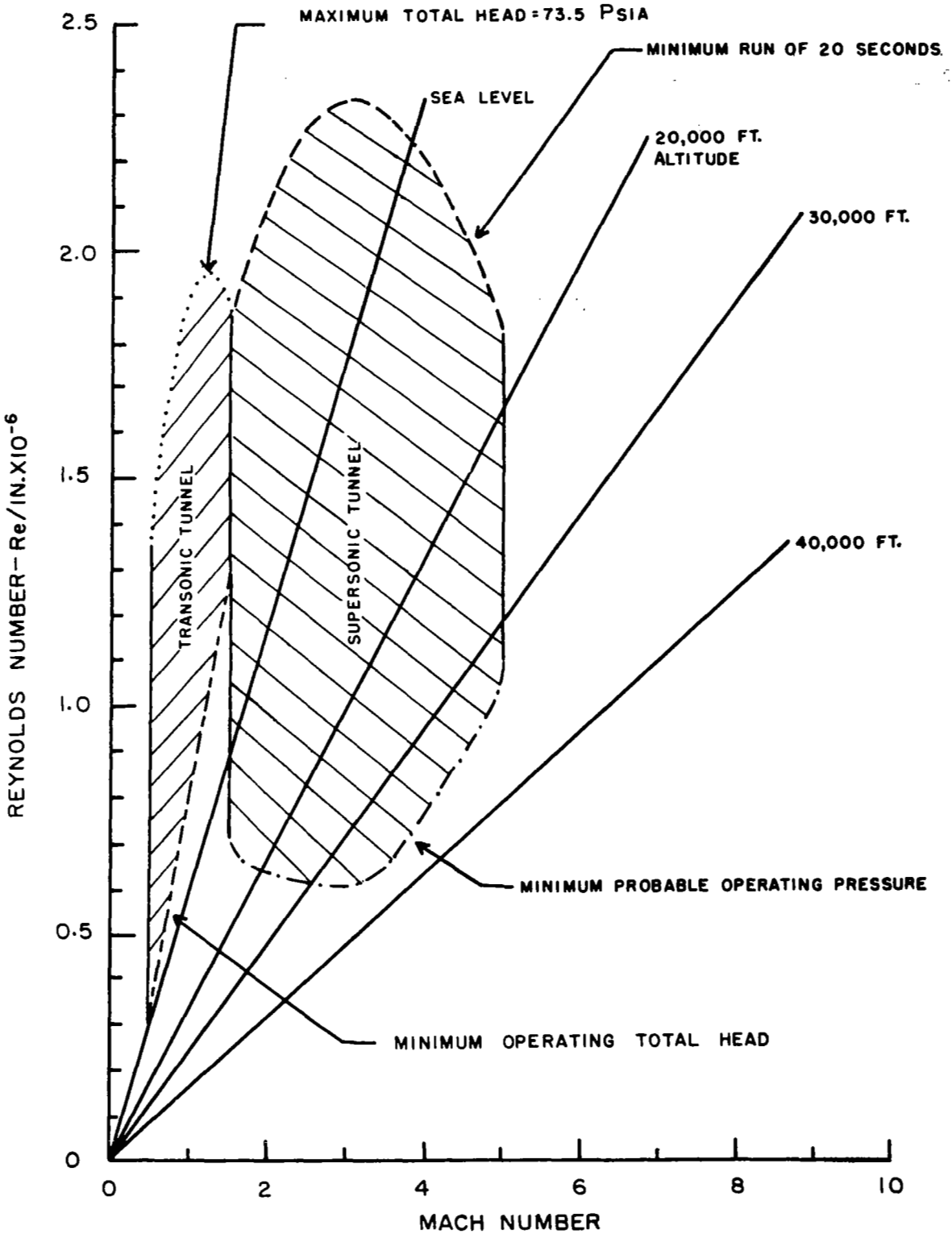

Figure 13. Reynolds Number Versus Mach Number and Altitude for Intermittent Flow Wind Tunnels

2. Special Equipment

Several types of special equipment were utilized during the test program to record the "buzz" frequency and pressure amplitude of the inlet model. A Tektronix type oscilloscope was connected to a differential pressure transducer mounted at the compressor face, station 7. This unit was completely self contained and required no external equipment other than the transducer. Excitation voltage for the strain gage type transducer was provided by a plug-in unit. The transducer consisted of a four strain gage bridge having a range 50 psi differential and a frequency response of 5. 1 KC. The duration of the oscilloscope trace was limited for the length of trace required. A complete trace from throttling through the "buzz" sequence was desirable. Therefore, subsequent runs were made on various types of oscillographs, (i. e. Sanborn and Visicorder). The Sanborn type oscillograph was a mechanical galvanometer direct writing recorder which provided a continuous trace of the test run. The Visicorder was a multichannel, general-purpose oscillograph direct recording instrument. It is commonly referred to as a light beam interrupter-type identifier.

A high speed rotating prism camera (Fastax) was used on several selected configurations to record the actual physical movements of the expelled shock through the schlieren system. This is the type of camera where the film and the image are moving at the same speeds due to the rotation of a prism within the camera. The film speed was approximately 1500 frames per second. A Polaroid still camera was also connected to the Schlieren visualization system to record the shock structure. This was accomplished by connecting the shutter system of the camera to the spark source allowing the spark to be tripped whenever the shutter was opened. The exposure time of this camera was approximately four microseconds.

DATA ANALYSIS

The purpose of this test program was to establish the effects of operating a high performance external-internal (mixed) compression inlet in a region of influence of an adjacent inlet which is operating with its normal shock expelled and "buzzing". The inlets used were axisymmetric, movable centerbody inlets, capable of demonstrating the high performance characteristics which were desired.

The program was conducted in two phases (I and II) between which slight modifications were made to the models. For discussion, the complete experimental program can be divided into five main subjects. These will be discussed in detail as follows: (1) calibration of the basic inlets with no inlet interference effects, (2) determination of the steady state performance penalties of an operating inlet in the presence of an unstarted ("buzzing") inlet, (3) establishment of the line of demarcation between inlet to inlet interference and no inlet to inlet interference, (4) the effect of placing a plate between inlets, and (5) the measurement of "buzz" frequency and pressure amplitude as well as shock motion during "buzz" cycle.

Items 1 and 3 were determined during both Phase I and Phase II. Item 2 was determined during Phase I of the test program and the remainder was determined during Phase II.

1. Calibration of the Basic Inlet

The inlet configuration was selected from previous tests because of its generally good performance over the Mach number range from Mo = 2.0 to Mo = 3.0. Figures 14, 15, 16 and 17 are presented showing the pressure recovery, mass flow ratio, centerbody bleed and contraction ratio of the reference inlet. Also shown with the reference inlet is the performance of the smaller scale inlet used in this test program. In Phase I, the cowl boundary layer was bled from the aft 10 rows of cowl perforations. In Phase II, the front 10 rows of cowl perforations were used.

In scaling the 4.5 inch diameter reference inlet to the 2.4 inch diameter inlets used in this program, the perforation diameter could not be scaled because of practical machining problems. During the Phase I testing, it was noted that large amounts of airflow spillage were present at Mach 3.0 as the peak recovery was approached during the throttling of the inlet airflow. It was further noted that the large decrease in mass flow ratio

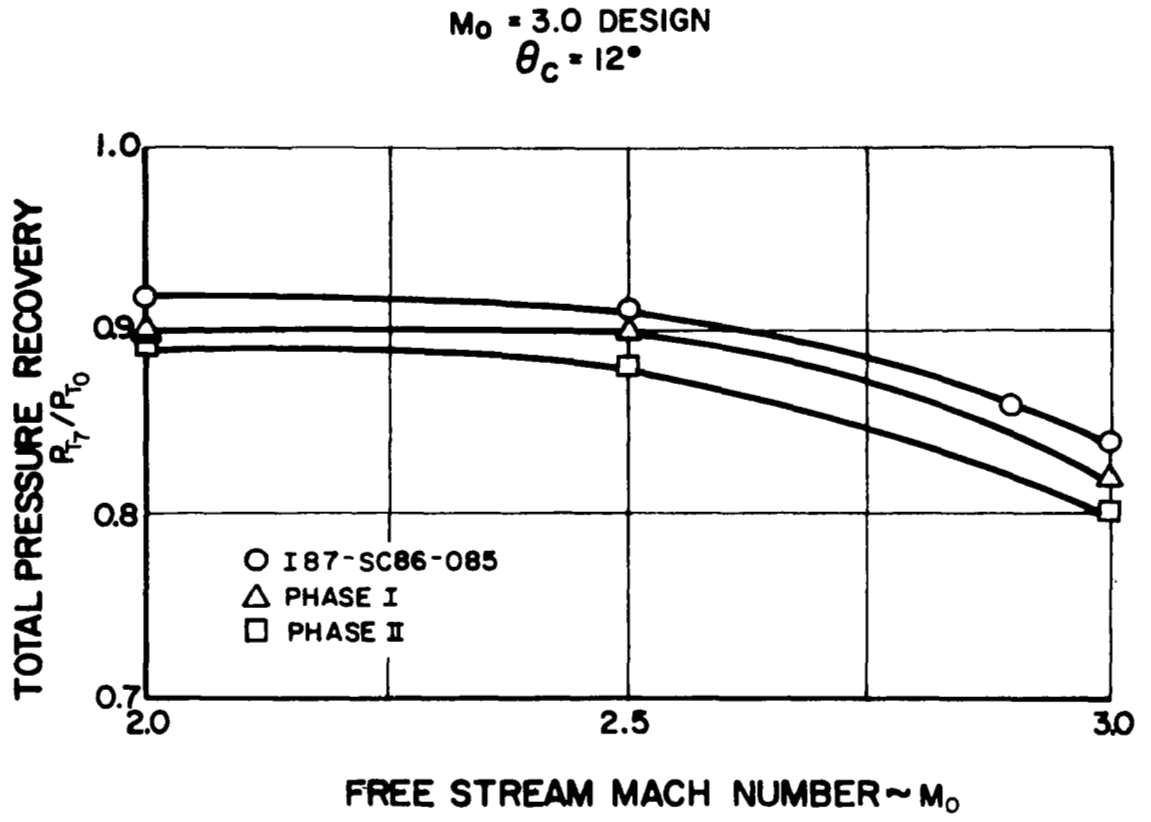

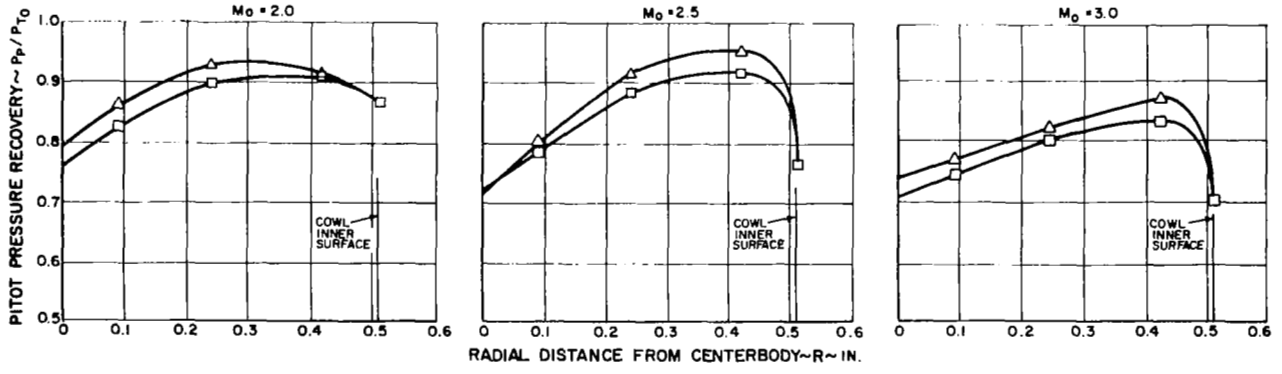

Figure 14. Variation of Total Pressure Recovery With Free Stream Mach Number and Compressor Face Pitot Pressure Profiles

was occurring as the normal shock approached the throat region and forced larger amounts of flow through the cowl perforations. This increased bleed produced a subsequent reduction in the overall aerodynamic contraction ratio. The testing in Phase II was accomplished utilizing the forward 10 rows of cowl perforation bleed by moving the last few rows out of the throat region to avoid this excess spillage. This caused a reduction in bleed, and an increase in contraction ratio, however very little change in pressure recovery resulted. Although the contraction ratio was low while using the downstream series of bleed perforations, the increased cowl bleed tended to compensate, probably because of an improved radial profile as shown in Figure 14. Apparently, the combination of the cowl bleed scale factor and the lower test Reynolds number for the 2.4 inch diameter inlets caused the slight reduction in the performance from the reference inlet. However, the performance was sufficiently high to establish realistic interference effects, since both inlets were operating with large amounts of internal contraction.

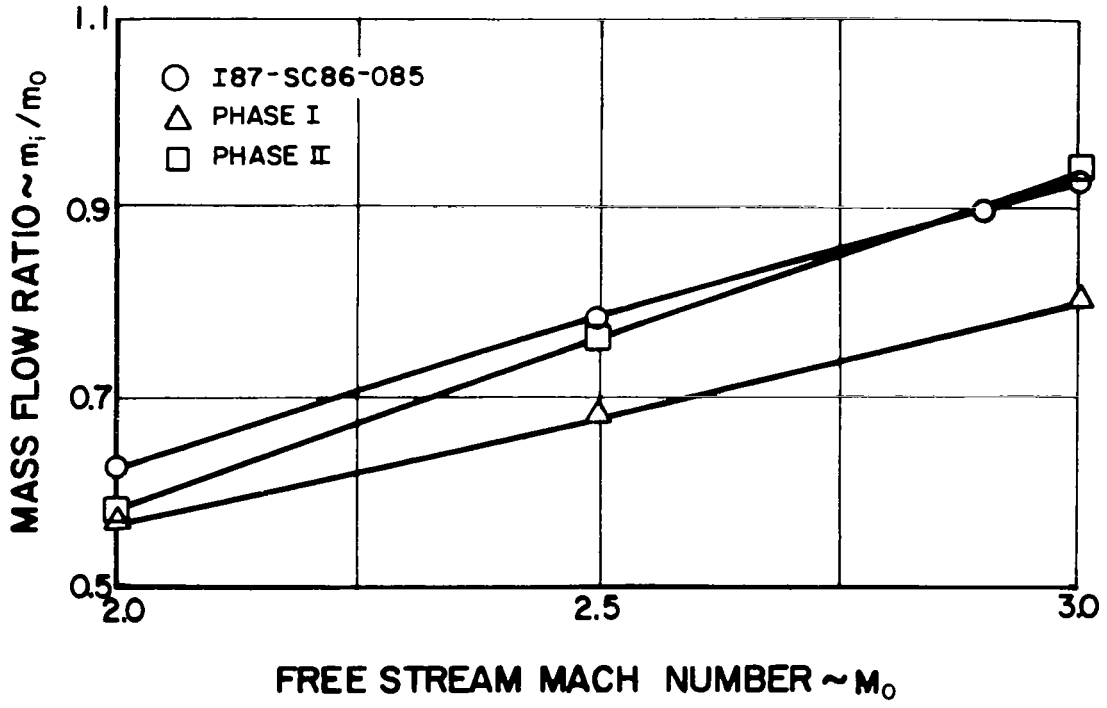

Figure 15. Variation of Mass Flow Ratio With Free Stream Mach Number - Mach 3.0 Design - $\Theta_c = 12°$

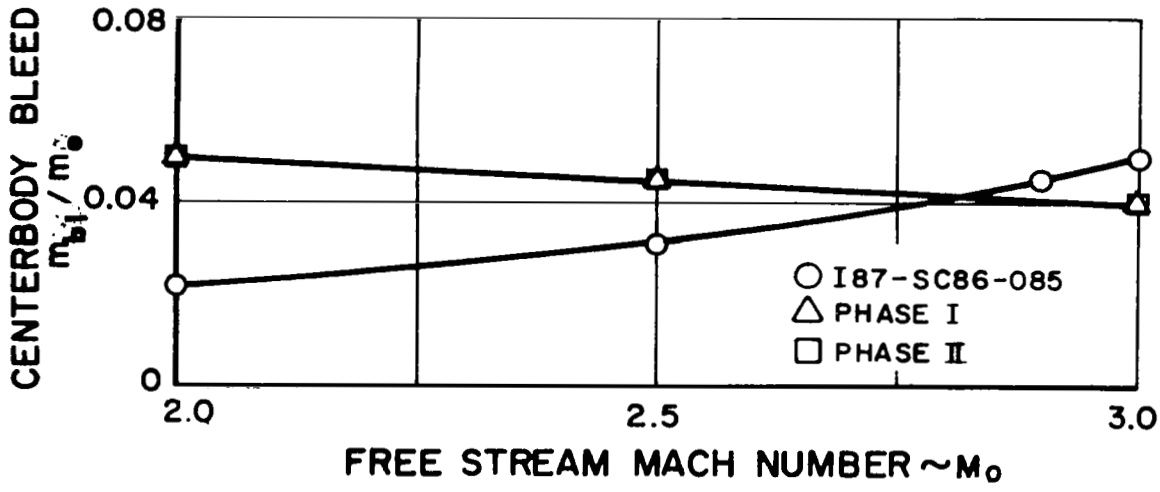

Figure 16. Variation of Centerbody Bleed With Free Stream Mach Number - Mach 3.0 Design - Θ_c = 12°

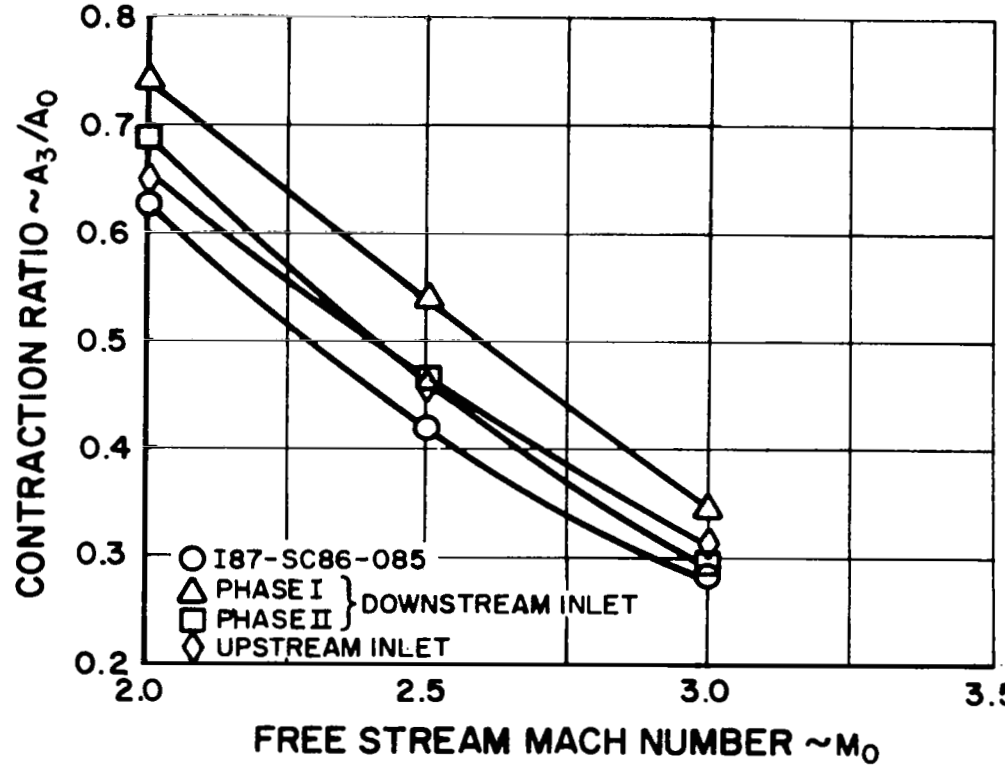

Figure 17. Contraction Ratio Versus Free Stream Mach Number

The data shown in Figures 14, 15 and 16 are for the downstream inlet only. The contraction ratio of the upstream inlet is shown in Figure 17 where it can be seen that only slight differences were present between the upstream and downstream inlets. The contraction ratio for the downstream inlet was determined from the measured mass flow ratio passing the compressor face station (see Figure 15) and the throat area ratio associated with a measured centerbody position (See Figure 5). It therefore does not take into account any mass flow bled off between the throat and the compressor face. The Phase I inlet configuration had some cowl bleed perforations between the throat and the compressor face and therefore the contraction ratios shown in Figure 17 for Phase I are somewhat misleading. Since the cowl bleed was not metered, it is not possible to make an allowance for this discrepancy, however; it will probably account for most of the difference between the Phase I and II contraction ratios shown in Figure 17. The contraction ratio of the upstream inlet was determined by using the measured centerbody position to obtain (1) overall mass flow ratio from theoretical curves (see Figure 18), and (2) the throat area ratio from Figure 5. The throat mass flow was determined by assuming that the centerbody bleed (Figure 16) was the same for both inlets, and by subtracting this quantity from the overall mass flow. The cowl bleed was equal to zero. The following centerbody positions were used for both inlets as well as for the reference inlet.

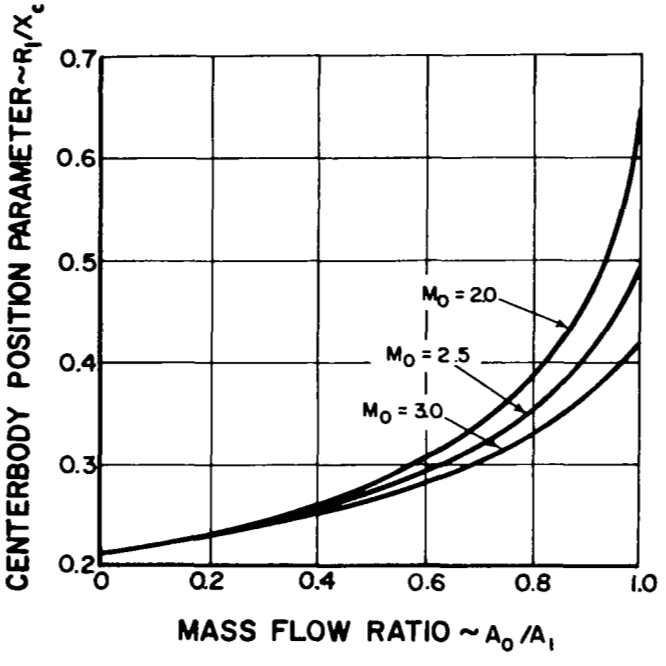

Figure 18. Theoretical Mass Flow Ratio as a Function of Centerbody Position

Centerbody Position (R_1/X_c)

	I87-SC86-085	Downstream Phase I	Downstream Phase II	Upstream
Mo = 2.0	.336	.316	.330	.328
Mo = 2.5	.378	.353	.362	.360
Mo = 3.0	.441	.423	.424	.413

As a point of interest, test points were attempted for Mo = 1.71 and 1.88 but the blockage and total pressure losses created by this relatively large frontal area per square inch of tunnel flow area would not allow the tunnel to remain started. Consequently, no valid test points were recorded below Mo = 2.0.

2. Determination of Performance Penalties

The intent of this experimental program was to map out the penalties for operating an inlet at several locations in the region of influence of an unstable inlet. At several Mach numbers, various combinations of pod spacings were tested to determine the penalty loss which occurs when operating in this condition. Figure 19 is a plot of the tested combinations and shows the performance loss as a function of the displacement distance parameter from the inlet to the expelled shock, G/D_1. The displacement distance parameter, G/D_1, is defined as the axial distance measured from the inboard leading edge of the downstream inlet cowl lip to the intersection of the "no-penalty" line at the specific pod spacing, ψ . This "no-penalty" line is shown in Figure 20 for various free stream Mach numbers and is the line which represents the maximum forward travel position of the expelled shock. A more descriptive analysis of this "no-penalty" line is given in the succeeding section entitled, "Establishment of the No Interference Penalty Line."

The procedure used to establish the pressure recovery penalties shown in Figure 19 was to, first cause the upstream inlet shock to become expelled by throttling the inlet airflow (throttle P), then re-establish a new maximum contraction ratio for the downstream inlet. The pressure recovery and mass flow ratio for the downstream inlet was then obtained with the upstream inlet's shock "buzzing". This procedure was repeated for variations in pod spacing from 1.0 inlet diameter to 3.0 inlet diameters, and for the Mach number range Mo=2.0 to 3.0.

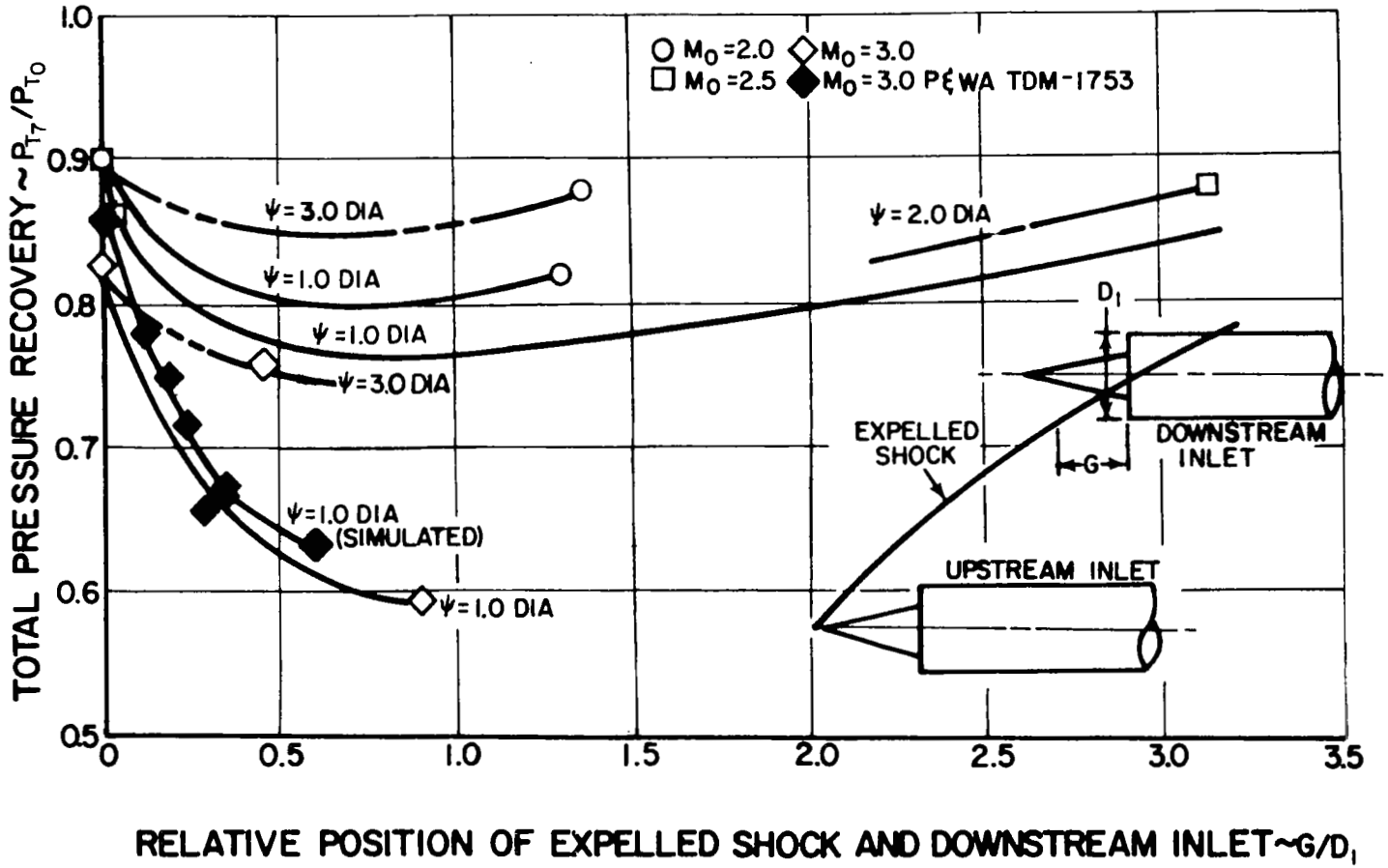

Figure 19. Downstream Inlet Pressure Recovery When Operating With Upstream Inlet Shock Expelled

An examination of the data of Figure 19 shows several trends. The greater the distance away from the source of the expelled shock, the less the penalty. At Mach 3.0, for instance, the maximum penalty at ψ = 1.0 diameter was approximately 22 percent relative to the no interference performance. An increase in spacing to ψ = 3.0 diameters reduces this penalty to approximately 7 percent. It is evident that the strength of the expelled shock plays an important role in the determination of the magnitude of the penalty. A similar trend is also noted at the other Mach numbers.

As the distance away from the expelled shock is increased, by increasing the axial spacing for a given lateral pod spacing, the penalty gets initially more severe until it reaches a maximum value. However, as the distance is further increased, the penalty is lessened, until at very great distances, it is apparent that no penalty will be incurred. The trends noted agree very well with the preliminary data recorded in Pratt & Whitney Aircraft report TDM 1753 (reference 1).

The results of Figure 19 further show that as the free stream Mach number is reduced, the maximum penalty incurred is also lessened.

The trends noted lead to the conclusion that the weaker the interference shock, either from lower free stream Mach numbers or greater distances from the source, the less the operating penalty. Such a conclusion is not contrary to the normal trend in supersonic flow.

An interesting aspect of the above test results is that the mass flow ratio of the downstream inlet did not vary more than 1 to 2 percent from the values obtained with no interference, even though the centerbody position parameter, R_1/X_c, and the pressure recovery did vary. R_1/X_c is tabulated as follows for the various points shown in Figure 19.

Mo	ψ	R_1/X_c
2.0	1.0	.319
2.0	3.0	.306
2.5	1.0	.364
2.5	2.0	.324
3.0	1.0	.364
3.0	3.0	.397

It should be emphasized that the results of Figure 19 indicate the performance levels which can be maintained by the downstream inlet with the upstream inlet "buzzing", after the initial shock expulsion of the upstream inlet. This would represent a condition on an aircraft where restarting of the upstream inlet was not possible through a control or mechanical malfunction.

The transient effect of unstarting the upstream inlet was found to impose a much more severe operating penalty. The upstream inlet was restarted while the downstream inlet remained operating at the contraction ratio previously determined with the upstream inlet "buzzing". However, as soon as the upstream inlet shock was expelled, the downstream inlet shock was also expelled. High performance inlets appear to be much more sensitive to a step change in pressure than to a continually fluctuating pressure (i. e., "buzzing"). This indicated that a much lower operating pressure recovery level would be required to allow for the most severe transient. It is possible that the amount of contraction in the downstream inlet could be reduced enough to prevent the shock from becoming expelled when operating in the unstable region, but, the resulting pressure recovery would most likely be too low to warrant locating inlets where this penalty must be imposed. It was, therefore, decided to forego further investigations of the penalties imposed in order to maintain operation of the downstream inlet at the instant of the shock expulsion of the upstream inlet, and to concentrate on the determination of the line of no interference penalty.

3. Establishment of the No Interference Penalty Line

Probably the most important information obtained in this experimental program was the establishment of the line of no interference, which distinguishes the region of stable and unstable operation of an inlet which is positioned near an adjacent inlet whose shock is expelled. The location of this operating line limit is needed in order to position inlet pods on supersonic aircraft without a penalty for interference.

The procedure used to establish this line was as follows: With the upstream inlet started (shock swallowed), the downstream inlet was operated at its maximum contraction ratio and throttled by the balance throttle, S, to approximately its peak pressure recovery. (These values were previously determined from the model calibration procedure, described fully in the model calibration section.) The upstream inlet shock was then expelled by throttling the airflow with throttle, P, resulting in the downstream inlet either remaining stable or going into a "buzzing" state. Due to the lack of a control system it was not possible to maintain exactly the peak pressure recovery on the downstream inlet and the normal sequence of running was to allow this inlet to run one to three percent supercritical. It was determined during this test program that this amount of supercritical operation did not have any noticeable effect on the stability of the inlet or the position of the no interference penalty line.

The tests were conducted at Mach 2.0, 2.5 and 3.0 for various lateral pod spacings, ψ , (1.0 to 3.0 inlet diameters) and axial distance parameters, Θ, (-5° to +70°).

The angle Θ is measured to the inboard edge of the cowl lip illustrated in phantom on Figure 20 at 68°. Figure 20 also shows the shape of the line of demarcation between inlet to inlet interference and no inlet to inlet interference. The test points are shown for both the stable and unstable operating points.

The no interference line continues to sweep back for constant Mach number until it approaches approximately a Mach line at the larger spacings. Note that although the shock is very weak at $\psi = 3.0$ diameters, its effect on inlet stability was still noted.

An interesting feature of these no interference lines is their similarity in shape for the various Mach numbers tested The displacement difference from Mach number to Mach number is approximately the same as the centerbody extension. This simplifies the requirements for the re-establishment of the line in the event that the model geometry is changed or the environmental flow conditions are different.

The shape of the no interference line approximates the most forward travel of the "buzzing" expelled shock. Figure 21 shows several shock positions which were photographed with a still camera through the Schlieren viewing system. A high speed light source stopped the buzzing shock in these various positions. It is interesting to note that the shock apparently does not move in and out in the same uniform manner during each "buzz" cycle. Only by coincidence would the still schlieren photos record the shock in its most forward position. Even the high speed movies, from which selected frames are shown for one "buzz" cycle in Figure 22, were not useable for getting an accurate location of this no interference line. The sensitivity of the inlet itself made the best indicator. The resulting shape when compared to the still photos and the high speed movies, tends to substantiate that it represents the envelope of the most forward positions encountered for the "buzzing" shock.

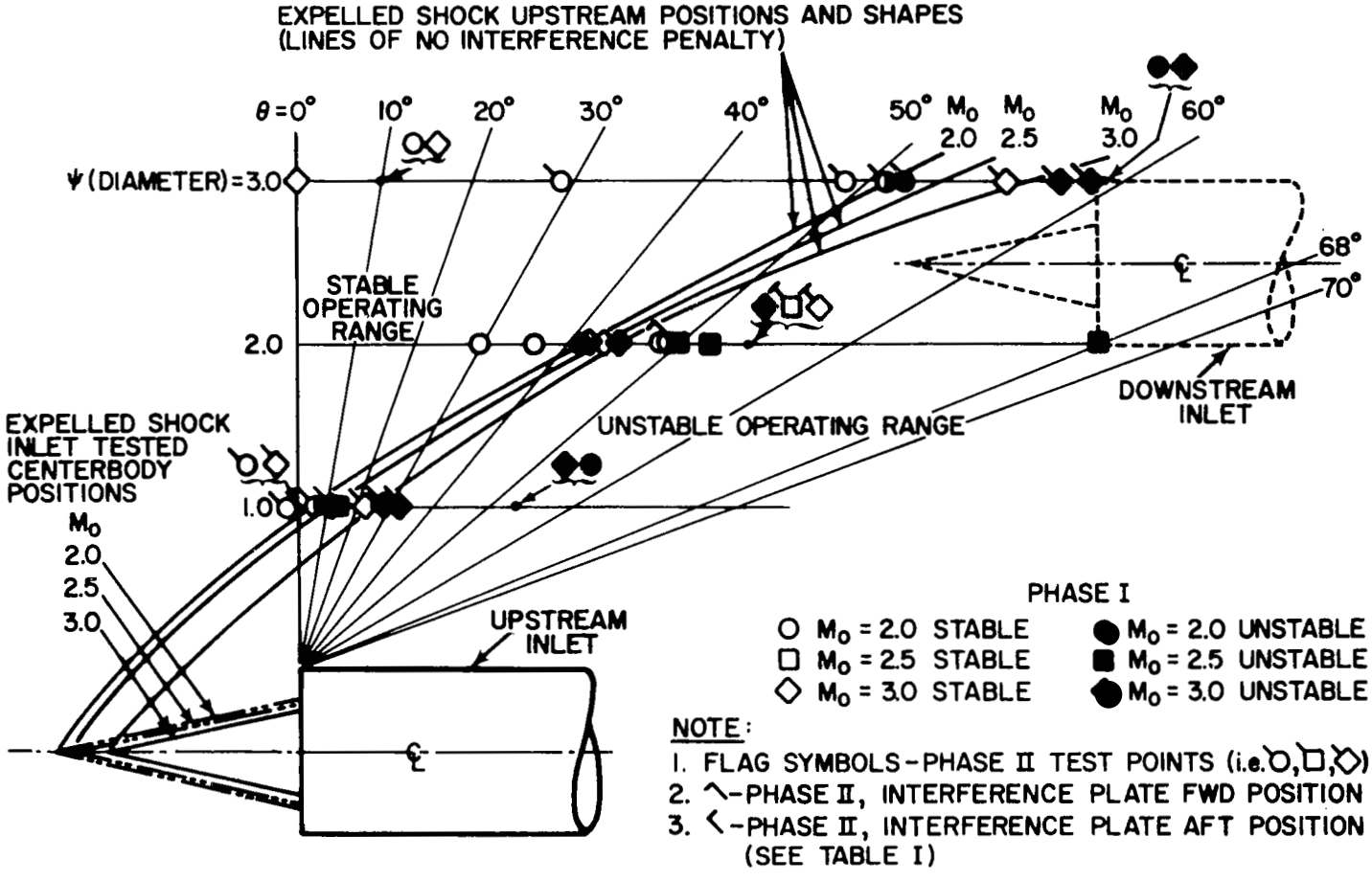

Figure 20. Test Results Showing Stability and Expelled Shock Positions and Shapes

TABLE 1

Tabulated Summary of Test Points
on Figure 20

ψ = 1.0 Diameter

Mo	θ	Phase	Conditions
2.0	-4°	II	stable
2.0	0°	II	stable
2.0	5°	II	marginal
2.0	54°	I	unstable
2.5	14.5°	I	unstable
3.0	0°	II	stable
3.0	12°	II	stable
3.0	22.5°	II	stable
3.0	28°	II	unstable
3.0	32°	II	unstable
3.0	54°	I	unstable

ψ = 2.0 Diameters

Mo	θ	Phase	Conditions
2.0	30°	I	stable
2.0	36.5°	I	stable
2.0	41.5°	I	marginal
2.0	48.5°	I	unstable
2.0	49°	II	stable - plate aft
2.5	49.5°	I	unstable
2.5	52.5°	I	unstable
2.5	55°	II	stable - plate aft
2.5	55°	II	stable - plate forward
2.5	68°	I	unstable
3.0	42°	I	stable
3.0	44°	I	stable
3.0	45°	I	marginal
3.0	55°	I	unstable

Mo	θ	Phase	Conditions
3.0	55°	II	stable - plate aft
3.0	55°	II	stable - plate forward

ψ = 3.0 Diameters

Mo	θ	Phase	Conditions
2.0	10°	I	stable
2.0	29°	II	stable
2.0	48.5°	II	stable
2.0	51°	II	marginal
2.0	51.5°	II	unstable
2.0	59.5°	I	unstable
3.0	0°	I	stable
3.0	10°	I	stable
3.0	56°	II	stable
3.0	58°	II	unstable
3.0	59°	II	unstable
3.0	59°	I	unstable

M_o = 3.0 ψ = 3.0 θ = 59°

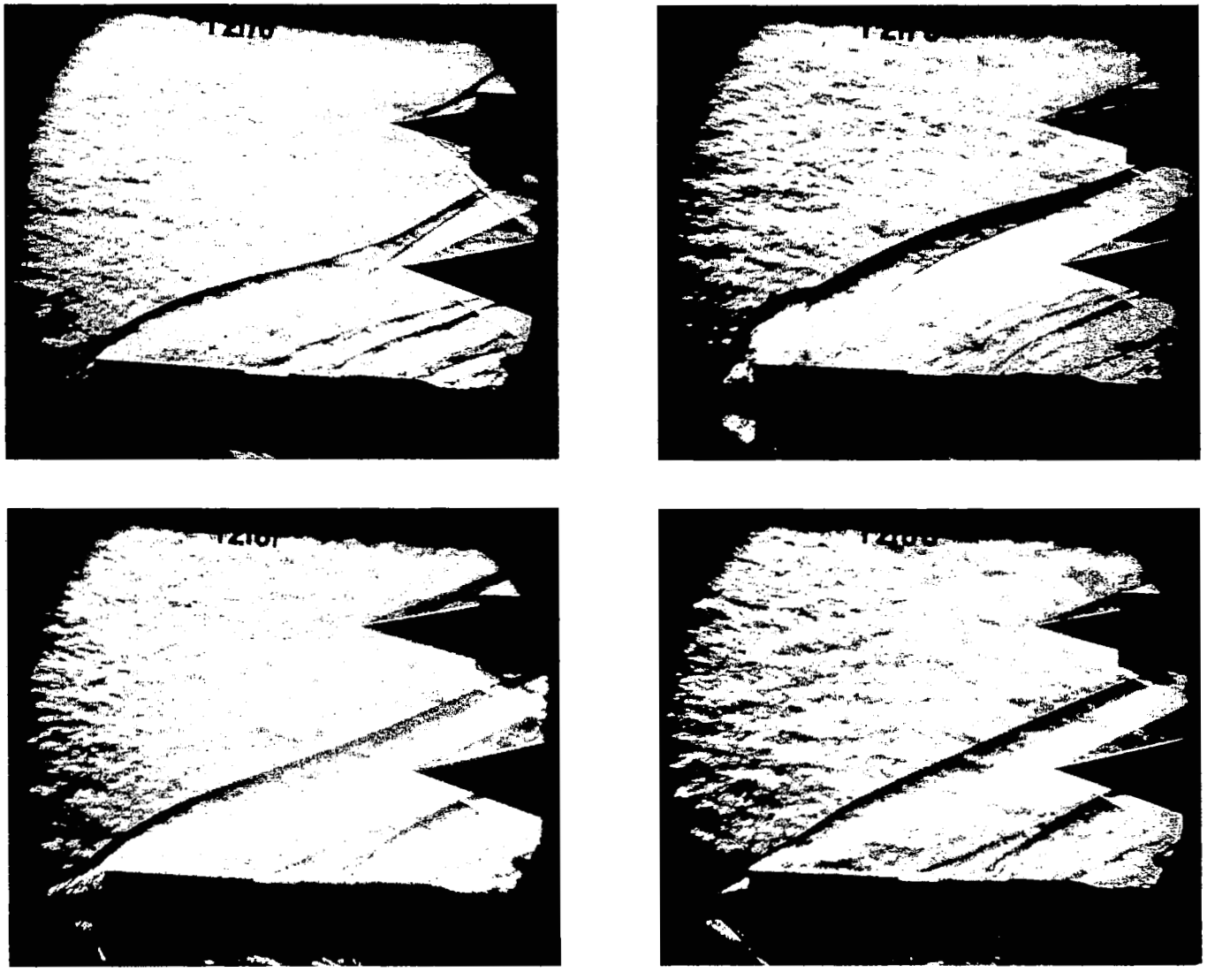

Figure 21. Selected Schlieren Photos Showing the Various Shock Shapes Encountered During "Buzz" Cycles

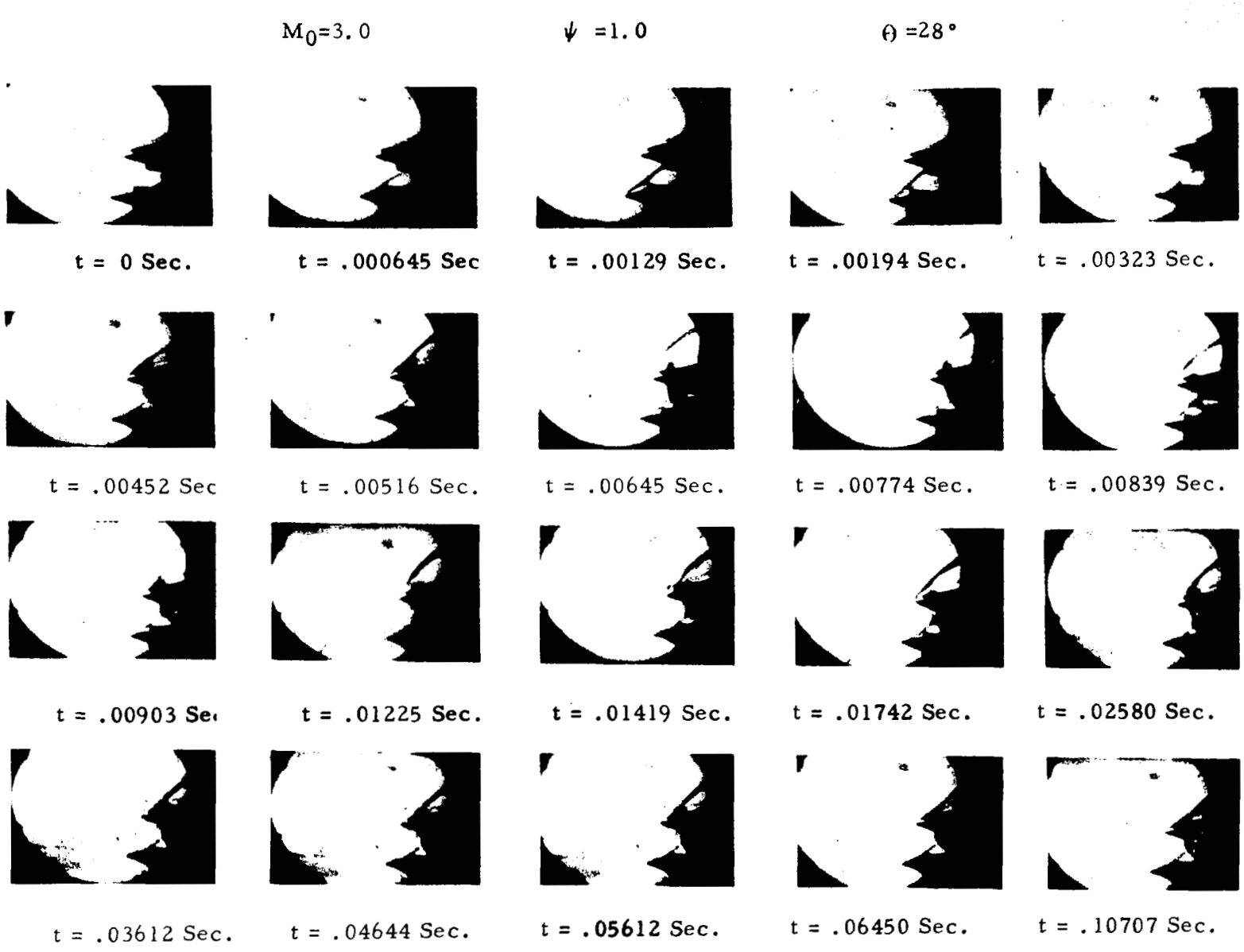

Figure 22. Selected Frames From High Speed Schlieren Movies Showing Expelled Shock Motion

4. The Effect of the Interference Plate

Following the establishment of the unstable region of operation, an attempt was made to shield the downstream inlet from the expelled shock of the upstream inlet by using an interference plate. Figure 23 illustrates the effectiveness of this plate. Without the plate, interference was present which unstarted the downstream inlet when it was operated at maximum contraction. When the plate was positioned between the inlets as a shield, the downstream inlet was allowed to operate normally. It was discovered that continued throttling of the upstream inlet (throttle P) after shock expulsion, caused the expelled shock to spill out around the leading edge of the plate. When this occurred, the downstream inlet became unstable. An extension of the interference plate to a further upstream position, allowed for additional throttling before the downstream inlet became unstable. Apparently, this plate would have to be tailored in size and spacing from the cowl in order to assure the best results. Figure 24 illustrates, with selected frames from a high speed schlieren movie, the shock motion for both a partially throttled condition and for the condition which eventually triggered the downstream inlet. The effect of the plate was tested at both Mo = 2.5 and 3.0 and found to have essentially the same characteristics.

At both Mach numbers, the centerbody shock reflected from the plate and back to the cowl well behind the cowl lip. No change in contraction ratio of the upstream inlet was noted. In the event a plate is used as a shield, care must be taken to prevent the centerbody shock from reflecting back into the inlet as this will surely affect the started performance of the inlet.

$M_o = 3.0$

ψ = 2.0 Dia. $\theta = 50.5^o$

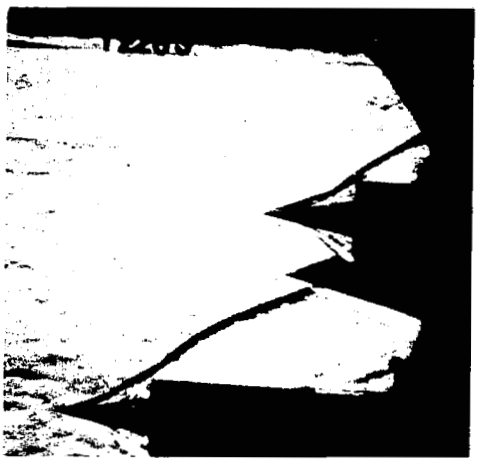

No Plate
(Unstable)

ψ = 2.0 Dia. $\theta = 55^o$

Plate in Aft Position
(Stable)

$M_o = 2.5$

ψ = 2.0 Dia. $\theta = 52.5^o$

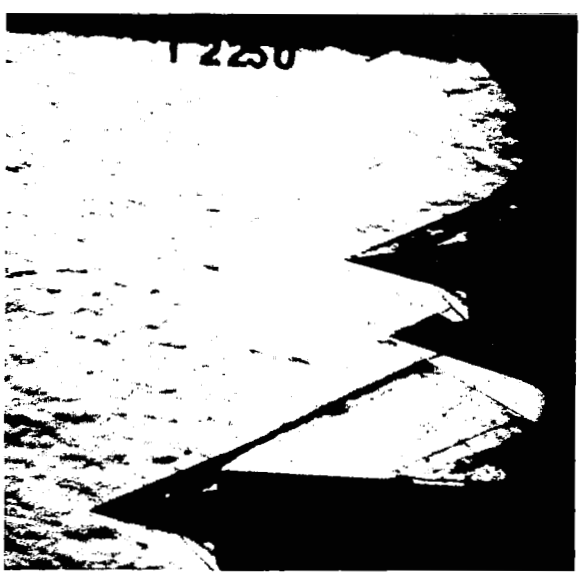

No Plate
(Unstable)

ψ = 2.0 Dia. $\theta = 55^o$

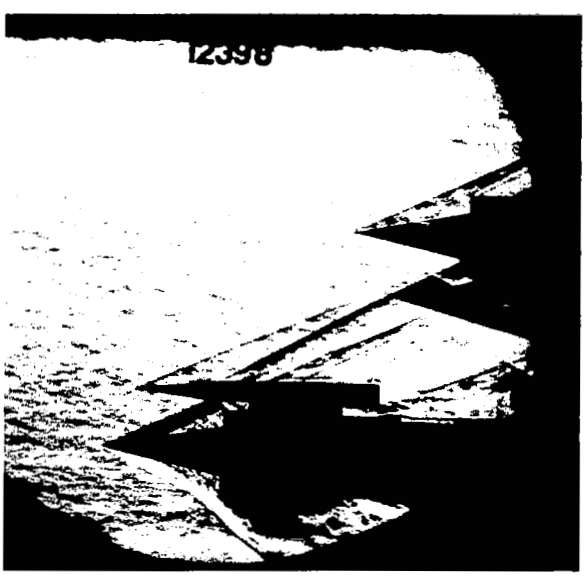

Plate in Forward Position
(Stable)

Figure 23. Schlieren Photographs Showing the Effectiveness of the Interference Plate

M_0=3.0 ψ=2.0 θ=54°

Upstream Inlet Shock Becomes Expelled, Downstream Inlet Stable

---

Further Reduction of Upstream Inlet Airflow

Downstream Inlet Shock Is Finally Expelled

Figure 24. Selected Frames From High Speed Schlieren Movies Showing Effects of Interference Plate on Downstream Inlet Stability

5. "Buzz Analysis"

During the Phase II testing, "buzz" frequency, pressure amplitude, and shock motion were recorded for the downstream inlet between Mach 2.0 to 3.0. The "buzz" frequency and pressure amplitude were recorded by oscilloscopes and oscillographs. The shock motion was also recorded by a high speed camera described in the test equipment section. The pressure variations were measured with a differential transducer close coupled to the model to eliminate lag.

It was initially assumed that the "buzz" frequency and pressure amplitude would be dependent on the volume between the cowl lip and the inlet throat and therefore be the same for both models. Analysis of the "buzz" frequencies showed that this was not the case. By observing the inlet expelled shock motion in the high speed schlieren movies the "buzz" frequency was seen to cycle at a much faster rate for the upstream inlet than for the downstream inlet. Because the next flow restriction which is encountered in the model takes place at the choked mass flow throttle, it was deduced that the frequency was dependent upon the volume between the cowl lip and this throttle. This volume was much less for the upstream inlet than for the downstream inlet and therefore probably accounts for the fact that the upstream inlet frequency was approximately twenty times the frequency of the downstream inlet.

In the early stages of the "buzz" measurement phase it was found that the oscilloscope would not completely record the pressure trace. This was due to the scale factor which was available on the oscilloscope. Therefore in order to determine the complete "buzz" frequency and amplitude for the initial transient as well as subsequent cycles, the oscilloscope was replaced by an oscillograph for the remaining runs.

The "buzz" frequency and pressures are shown for the downstream inlet at Mach 2.0 and Mach 3.0 in Figure 25. It can be seen from this figure that the "buzz" frequencies are approximately the same for both Mach numbers and that the only variation is in the pressure amplitude. This might be explained by the difference in the contraction ratios or the total pressure recoveries between these two Mach numbers. The amplitude at Mo = 2.0 is approximately 28 percent of the free stream total pressure and at Mo = 3.0 it is approximately 12 percent of the total pressure. Figure 26 shows that the amplitude at Mo = 2.5 is approximately the same as the Mo = 2.0 amplitude. The peak total pressure recoveries at Mach 2.0 and 2.5 are also approximately equal (See Figure 14).

Figure 26 also shows the effect of throttling the inlet airflow on the "buzz" frequency. During this run the frequency increased from six c.p.s. to approximately nine c.p.s. It should be noted that although the frequency changed during throttling, the amplitude remained approximately constant. This trend indicates that although the "buzz" frequency on the upstream inlet was higher than the downstream inlet, it can be assumed that the pressure amplitude remained approximately the same. Due to the lack of instrumentation on the upstream model, this assumption could not be verified.

Figure 22 shows selected frames from the high speed schlieren movies with the time indicated for each frame. Note that the shock from the downstream inlet is not expelled by the upstream expelled shock until a finite elapsed time has occurred (i.e. frame 4 to frame 6). Note also that the shock remains at its inner most position for a significantly longer time than it does at its maximum upstream position. The oscillograph trace in Figure 26 tends to verify this fact. It is also interesting to note in the pressure trace that the magnitude of the minimum pressure obtained in the initial transient pressure drop is the same as the pressure in subsequent cycles. The amplitude for all cycles is also a constant.

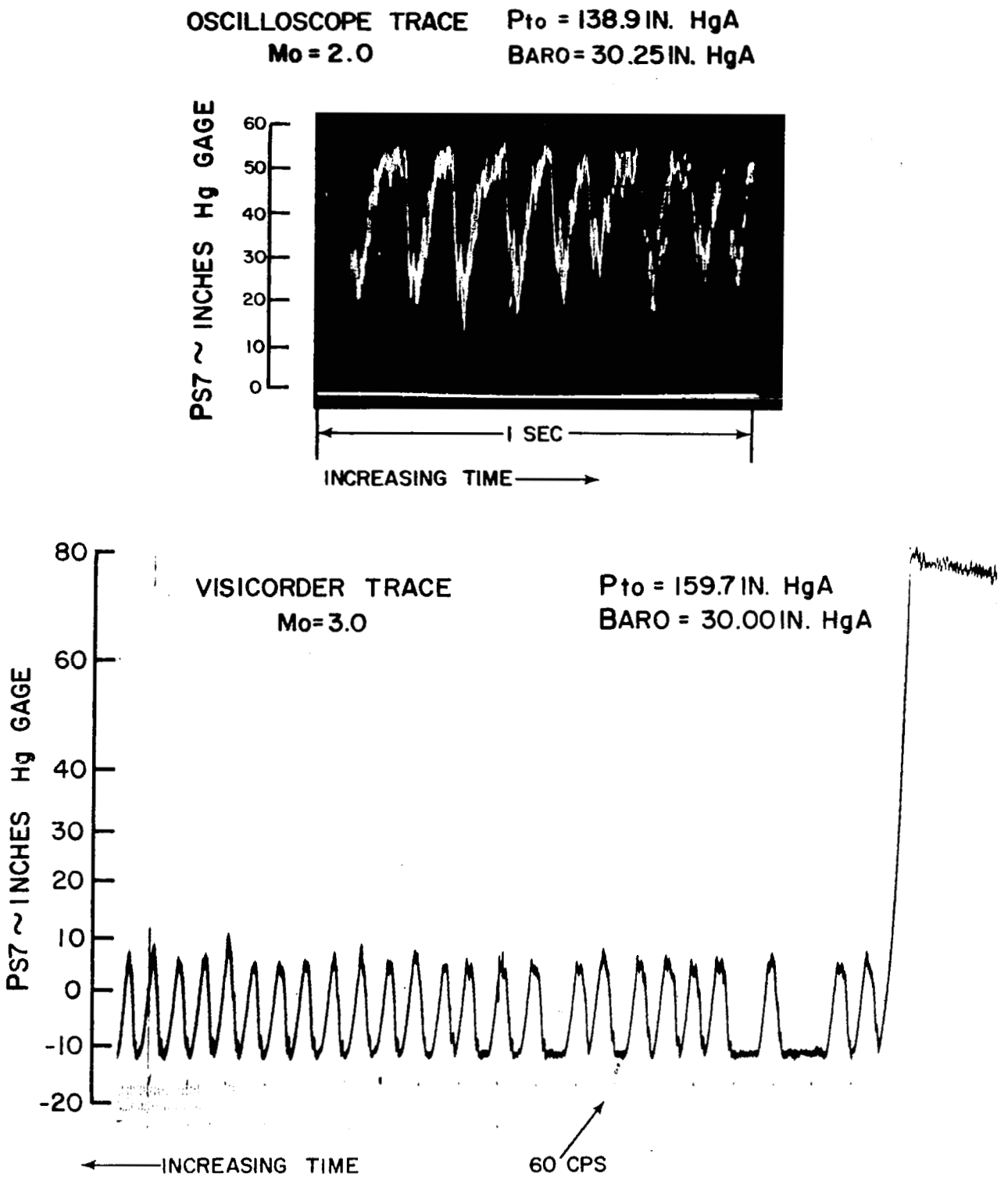

Figure 25. Oscilloscope and Oscillograph Tracings Showing "Buzz" Frequency and Pressure Amplitude

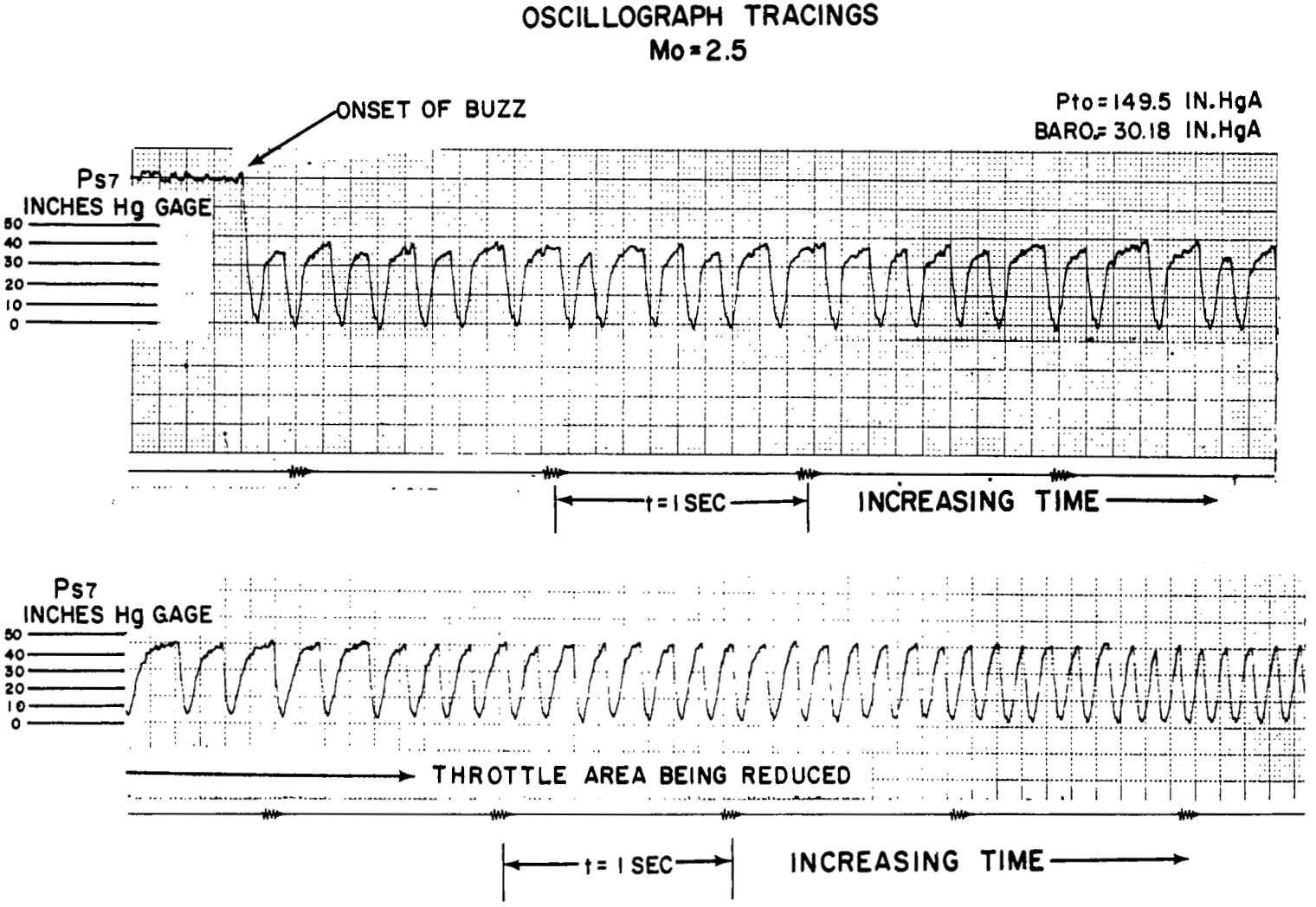

Figure 26. Oscillograph Tracings Showing "Buzz" Frequency and Pressure Amplitude

Recommendations

1. Based on the magnitude of the penalties which are encountered in the region of expelled shock interference, it is recommended that the pods of a supersonic aircraft be located so that no interference will be experienced while the inlet operates with internal compression. The best arrangement for satisfying this condition is to place the pods with the cowl lips in the same plane and spaced at least 1.0 diameters apart. Probably 1.5 diameters would be better to allow for a margin of safety.

   In order to position pods in the interference region so that the penalty would be a minimum the spacing required would be so great that they would probably be farther apart than the aircraft structure would allow.

2. In testing the plate which was used as an interference shield it was evident that this plate should be tailored to fit the specific application. It is recommended that further work be done to investigate the minimum plate size and optimum plate location which might be possible.

3. Because the maximum upstream position of the expelled normal shock defines the line of no interference, it is recommended that this information be recorded in future tests of all inlets with internal contraction. One very simple means of obtaining information of this type could be to take a time exposure on a single film plate during the 'buzz' operation. The envelope of the blurred shock image should show the maximum forward position of the expelled shock.

REFERENCES

1. Motycka, D. L.: The Effect of an Interference Shock on the Performance of a Mach 3.0 Axisymmetric Movable Centerbody Inlet. Pratt & Whitney Aircraft Report TDM-1753, January, 1962.

2. Trimpi, Robert L: Air Analysis of Buzzing in Supersonic Ram Jets by a Modified One-Dimensional Nonstationary Wave Theory. NACA Technical Note 3695, July, 1956.

3. Mirels, Harold: Acoustic Analysis of Ram Jet Buzz. NACA Lewis Flight Propulsion Laboratory, NACA Technical Note 3574, November, 1955.

4. Sterbentz, W. H. and Davids, J.: Amplitude of Supersonic Diffuser Flow Pulsations. NACA Technical Note 3572, October, 1955.

5. Sterbentz, W. H. and Evvard, J. C.: Criterions for Prediction and Control of Ram-Jet Flow Pulsations. NACA Technical Note 3506, August, 1955.

6. McLafferty, G. H. and Vergara, R. D.: Description of Equipment and Techniques Used for Inlet Tests in UAC Research Department 17-inch Blowdown Tunnels. UAC Research Laboratories Report R-2000-30, July, 1957.